

This discussion paper is/has been under review for the journal Earth System Science Data (ESSD). Please refer to the corresponding final paper in ESSD if available.

## Global carbon budget 2014

C. Le Quéré<sup>1</sup>, R. Moriarty<sup>1</sup>, R. M. Andrew<sup>2</sup>, G. P. Peters<sup>2</sup>, P. Ciais<sup>3</sup>,  
P. Friedlingstein<sup>4</sup>, S. D. Jones<sup>1</sup>, S. Sitch<sup>5</sup>, P. Tans<sup>6</sup>, A. Arneth<sup>7</sup>, T. A. Boden<sup>8</sup>,  
L. Bopp<sup>3</sup>, Y. Bozec<sup>9,10</sup>, J. G. Canadell<sup>11</sup>, F. Chevallier<sup>3</sup>, C. E. Cosca<sup>12</sup>, I. Harris<sup>13</sup>,  
M. Hoppema<sup>14</sup>, R. A. Houghton<sup>15</sup>, J. I. House<sup>16</sup>, A. Jain<sup>17</sup>, T. Johannessen<sup>18,19</sup>,  
E. Kato<sup>20</sup>, R. F. Keeling<sup>21</sup>, V. Kitidis<sup>22</sup>, K. Klein Goldewijk<sup>23</sup>, C. Koven<sup>24</sup>,  
C. S. Landa<sup>18,19</sup>, P. Landschützer<sup>25</sup>, A. Lenton<sup>26</sup>, I. D. Lima<sup>27</sup>, G. Marland<sup>28</sup>,  
J. T. Mathis<sup>12</sup>, N. Metz<sup>29</sup>, Y. Nojiri<sup>20</sup>, A. Olsen<sup>18,19</sup>, T. Ono<sup>30</sup>, W. Peters<sup>31</sup>,  
B. Pfeil<sup>18,19</sup>, B. Poulter<sup>32</sup>, M. R. Raupach<sup>33</sup>, P. Regnier<sup>34</sup>, C. Rödenbeck<sup>35</sup>,  
S. Saito<sup>36</sup>, J. E. Salisbury<sup>37</sup>, U. Schuster<sup>5</sup>, J. Schwinger<sup>18,19</sup>, R. Séférian<sup>38</sup>,  
J. Segsneider<sup>39</sup>, T. Steinhoff<sup>40</sup>, B. D. Stocker<sup>41</sup>, A. J. Sutton<sup>42,12</sup>,  
T. Takahashi<sup>43</sup>, B. Tilbrook<sup>44</sup>, G. R. van der Werf<sup>45</sup>, N. Viovy<sup>3</sup>, Y.-P. Wang<sup>46</sup>,  
R. Wanninkhof<sup>47</sup>, A. Wiltshire<sup>48</sup>, and N. Zeng<sup>49</sup>

<sup>1</sup>Tyndall Centre for Climate Change Research, University of East Anglia, Norwich Research Park, Norwich NR4 7TJ, UK

<sup>2</sup>Center for International Climate and Environmental Research – Oslo (CICERO), Norway

<sup>3</sup>Laboratoire des Sciences du Climat et de l'Environnement, CEA-CNRS-UVSQ, CE Orme des Merisiers, 91191 Gif sur Yvette Cedex, France

<sup>4</sup>College of Engineering, Mathematics and Physical Sciences, University of Exeter, Exeter, EX4 4QF, UK

521

<sup>5</sup>College of Life and Environmental Sciences, University of Exeter, Exeter, EX4 4QE, UK

<sup>6</sup>National Oceanic & Atmospheric Administration, Earth System Research Laboratory (NOAA/ESRL), Boulder, Colorado 80305, USA

<sup>7</sup>Karlsruhe Institute of Technology, Institute of Meteorology and Climate Research/Atmospheric Environmental Research, 82467 Garmisch-Partenkirchen, Germany

<sup>8</sup>Carbon Dioxide Information Analysis Center (CDIAC), Oak Ridge National Laboratory, Oak Ridge, TN, USA

<sup>9</sup>CNRS, UMR7144, Equipe Chimie Marine, Station Biologique de Roscoff, Place Georges Teissier, 29680 Roscoff, France

<sup>10</sup>Sorbonne Universités (UPMC, Univ Paris 06), UMR7144, Adaptation et Diversité en Milieu Marin, Station Biologique de Roscoff, 29680 Roscoff, France

<sup>11</sup>Global Carbon Project, CSIRO Oceans and Atmosphere Flagship, GPO Box 3023, Canberra, ACT 2601, Australia

<sup>12</sup>National Oceanic & Atmospheric Administration/Pacific Marine Environmental Laboratory (NOAA/PMEL), 7600 Sand Point Way NE, Seattle, WA 98115, USA

<sup>13</sup>Climatic Research Unit, University of East Anglia, Norwich Research Park, Norwich, NR4 7TJ, UK

<sup>14</sup>Alfred Wegener Institute Helmholtz Centre for Polar and Marine Research; Postfach 120161, 27515 Bremerhaven, Germany

<sup>15</sup>Woods Hole Research Centre (WHRC), Falmouth, MA 02540, USA

<sup>16</sup>Cabot Institute, Department of Geography, University of Bristol, Bristol BS8 1TH, UK

<sup>17</sup>Department of Atmospheric Sciences, University of Illinois, Urbana, IL 61821, USA

<sup>18</sup>Geophysical Institute, University of Bergen, Allégaten 70, 5007 Bergen, Norway

<sup>19</sup>Bjerknes Centre for Climate Research, Allégaten 55, 5007 Bergen, Norway

<sup>20</sup>Center for Global Environmental Research, National Institute for Environmental Studies (NIES), 16-2 Onogawa, Tsukuba, Ibaraki 305-8506, Japan

<sup>21</sup>University of California, San Diego, Scripps Institution of Oceanography, La Jolla, California 92093-0244, USA

<sup>22</sup>Plymouth Marine Laboratory, Prospect Place, Plymouth, PL1 3DH, UK

<sup>23</sup>PBL Netherlands Environmental Assessment Agency, The Hague/Bilthoven and Utrecht University, Utrecht, the Netherlands

522



## Abstract

Accurate assessment of anthropogenic carbon dioxide (CO<sub>2</sub>) emissions and their redistribution among the atmosphere, ocean, and terrestrial biosphere is important to better understand the global carbon cycle, support the development of climate policies, and project future climate change. Here we describe datasets and a methodology to quantify all major components of the global carbon budget, including their uncertainties, based on the combination of a range of data, algorithms, statistics and model estimates and their interpretation by a broad scientific community. We discuss changes compared to previous estimates, consistency within and among components, alongside methodology and data limitations. CO<sub>2</sub> emissions from fossil fuel combustion and cement production ( $E_{FF}$ ) are based on energy statistics and cement production data, respectively, while emissions from Land-Use Change ( $E_{LUC}$ ), mainly deforestation, are based on combined evidence from land-cover change data, fire activity associated with deforestation, and models. The global atmospheric CO<sub>2</sub> concentration is measured directly and its rate of growth ( $G_{ATM}$ ) is computed from the annual changes in concentration. The mean ocean CO<sub>2</sub> sink ( $S_{OCEAN}$ ) is based on observations from the 1990s, while the annual anomalies and trends are estimated with ocean models. The variability in  $S_{OCEAN}$  is evaluated with data products based on surveys of ocean CO<sub>2</sub> measurements. The global residual terrestrial CO<sub>2</sub> sink ( $S_{LAND}$ ) is estimated by the difference of the other terms of the global carbon budget and compared to results of independent Dynamic Global Vegetation Models forced by observed climate, CO<sub>2</sub> and land cover change (some including nitrogen-carbon interactions). *We compare the variability and mean land and ocean fluxes to estimates from three atmospheric inverse methods for three broad latitude bands.* All uncertainties are reported as  $\pm 1\sigma$ , reflecting the current capacity to characterise the annual estimates of each component of the global carbon budget. For the last decade available (2004–2013),  $E_{FF}$  was  $8.9 \pm 0.4 \text{ GtC yr}^{-1}$ ,  $E_{LUC}$   $0.9 \pm 0.5 \text{ GtC yr}^{-1}$ ,  $G_{ATM}$   $4.3 \pm 0.1 \text{ GtC yr}^{-1}$ ,  $S_{OCEAN}$   $2.6 \pm 0.5 \text{ GtC yr}^{-1}$ , and  $S_{LAND}$   $2.9 \pm 0.8 \text{ GtC yr}^{-1}$ . For year 2013 alone,  $E_{FF}$

525

grew to  $9.9 \pm 0.5 \text{ GtC yr}^{-1}$ , 2.3% above 2012, continuing the growth trend in these emissions.  $E_{LUC}$  was  $0.9 \pm 0.5 \text{ GtC yr}^{-1}$ ,  $G_{ATM}$  was  $5.4 \pm 0.2 \text{ GtC yr}^{-1}$ ,  $S_{OCEAN}$  was  $2.9 \pm 0.5 \text{ GtC yr}^{-1}$  and  $S_{LAND}$  was  $2.5 \pm 0.9 \text{ GtC yr}^{-1}$ .  $G_{ATM}$  was high in 2013 reflecting a steady increase in  $E_{FF}$  and smaller and opposite changes between  $S_{OCEAN}$  and  $S_{LAND}$  compared to the past decade (2004–2013). The global atmospheric CO<sub>2</sub> concentration reached  $395.31 \pm 0.10 \text{ ppm}$  averaged over 2013. We estimate that  $E_{FF}$  will increase by 2.5% (1.3–3.5%) to  $10.1 \pm 0.6 \text{ GtC}$  in 2014 ( $37.0 \pm 2.2 \text{ GtCO}_2 \text{ yr}^{-1}$ ), 65% above emissions in 1990, based on projections of World Gross Domestic Product and recent changes in the carbon intensity of the economy. From this projection of  $E_{FF}$  and assumed constant  $E_{LUC}$  for 2014, cumulative emissions of CO<sub>2</sub> will reach about  $545 \pm 55 \text{ GtC}$  ( $2000 \pm 200 \text{ GtCO}_2$ ) for 1870–2014, about 75% from  $E_{FF}$  and 25% from  $E_{LUC}$ . This paper documents changes in the methods and datasets used in this new carbon budget compared with previous publications of this living dataset (Le Quéré et al., 2013, 2014). All observations presented here can be downloaded from the Carbon Dioxide Information Analysis Center (doi:10.3334/CDIAC/GCP\_2014).

Italic font highlights significant methodological changes and results compared to the Le Quéré et al. (2014) manuscript that accompanies the previous version of this living data.

## 1 Introduction

The concentration of carbon dioxide (CO<sub>2</sub>) in the atmosphere has increased from approximately 277 parts per million (ppm) in 1750 (Joos and Spahni, 2008), the beginning of the Industrial Era, to 395.31 ppm in 2013 (Dlugokencky and Tans, 2014). Daily averages went above 400 ppm for the first time at Mauna Loa station in May 2013 (Scripps, 2013). This station holds the longest running record of direct measurements of atmospheric CO<sub>2</sub> concentration (Tans and Keeling, 2014; Fig. 1). The atmospheric CO<sub>2</sub>

526

increase above preindustrial levels was initially, primarily, caused by the release of carbon to the atmosphere from deforestation and other land-use change activities (Ciais et al., 2013). While emissions from fossil fuel combustion started before the Industrial Era, they only became the dominant source of anthropogenic emissions to the atmosphere from around 1920 and their relative share continued to increase until present. Anthropogenic emissions occur on top of an active natural carbon cycle that circulates carbon between the atmosphere, ocean, and terrestrial biosphere reservoirs on time scales from days to millennia, while exchanges with geologic reservoirs have even longer timescales (Archer et al., 2009).

The global carbon budget presented here refers to the mean, variations, and trends in the perturbation of CO<sub>2</sub> in the atmosphere, referenced to the beginning of the Industrial Era. It quantifies the input of CO<sub>2</sub> to the atmosphere by emissions from human activities, the growth of CO<sub>2</sub> in the atmosphere, and the resulting changes in the storage of carbon in the land and ocean reservoirs in response to increasing atmospheric CO<sub>2</sub> levels, climate change and variability, and other anthropogenic and natural changes (Fig. 2). An understanding of this perturbation budget over time and the underlying variability and trends of the natural carbon cycle are necessary to understand the response of natural sinks to changes in climate, CO<sub>2</sub> and land use change drivers, and the permissible emissions for a given climate stabilization target.

The components of the CO<sub>2</sub> budget that are reported in this paper include separate estimates for (1) the CO<sub>2</sub> emissions from fossil fuel combustion and cement production ( $E_{FF}$ ), (2) the CO<sub>2</sub> emissions resulting from deliberate human activities on land leading to Land-Use Change (LUC;  $E_{LUC}$ ), (3) the growth rate of CO<sub>2</sub> in the atmosphere ( $G_{ATM}$ ), and the uptake of CO<sub>2</sub> by the “CO<sub>2</sub> sinks” in (4) the ocean ( $S_{OCEAN}$ ) and (5) on land ( $S_{LAND}$ ). The CO<sub>2</sub> sinks as defined here include the response of the land and ocean to elevated CO<sub>2</sub> and changes in climate and other environmental conditions. The global emissions and their partitioning among the atmosphere, ocean and land are in balance:

$$E_{FF} + E_{LUC} = G_{ATM} + S_{OCEAN} + S_{LAND} \quad (1)$$

527

$G_{ATM}$  is usually reported in ppm yr<sup>-1</sup>, which we convert to units of carbon mass using 1 ppm = 2.120 GtC (Prather et al., 2012; Table 1). We also include a quantification of  $E_{FF}$  by country, computed with both territorial and consumption based accounting (see Methods).

Equation (1) partly omits two kinds of processes. The first is the net input of CO<sub>2</sub> to the atmosphere from the chemical oxidation of reactive carbon-containing gases from sources other than fossil fuels (e.g. fugitive anthropogenic CH<sub>4</sub> emissions, industrial processes, and changes of biogenic emissions from changes in vegetation, fires, wetlands, etc.), primarily methane (CH<sub>4</sub>), carbon monoxide (CO), and volatile organic compounds such as isoprene and terpene. The second is the anthropogenic perturbation to carbon cycling in terrestrial freshwaters, estuaries, and coastal areas, that modifies lateral fluxes from land ecosystems to the open ocean, the evasion CO<sub>2</sub> flux from rivers, lakes and estuaries to the atmosphere, and the net air-sea anthropogenic CO<sub>2</sub> flux of coastal areas (Regnier et al., 2013). These flows are omitted in absence of annual information on the natural versus anthropogenic perturbation terms of these loops of the carbon cycle, and they are discussed in Sect. 2.7. The inclusion of these fluxes of anthropogenic CO<sub>2</sub> would affect the estimates of, and partitioning between,  $S_{LAND}$  and  $S_{OCEAN}$  in Eq. (1) in complementary ways, but would not affect the other terms in Eq. (1).

The CO<sub>2</sub> budget has been assessed by the Intergovernmental Panel on Climate Change (IPCC) in all assessment reports (Ciais et al., 2013; Denman et al., 2007; Prentice et al., 2001; Schimel et al., 1995; Watson et al., 1990), and by others (e.g. Ballantyne et al., 2012). These assessments included budget estimates for the decades of the 1980s, 1990s (Denman et al., 2007) and, most recently, the period 2002–2011 (Ciais et al., 2013). The IPCC methodology has been adapted and used by the Global Carbon Project (GCP, www.globalcarbonproject.org), who has coordinated a cooperative community effort for the annual publication of global carbon budgets up to year 2005 (Raupach et al., 2007; including fossil emissions only), year 2006 (Canadell et al., 2007), year 2007 (published online; GCP, 2007), year 2008 (Le Quéré et al., 2009),

528





amount of flared or vented fuel. For emission years 2011–2013, flaring is assumed constant from 2010 (emission year) UN-based data. The basic data on gas flaring report atmospheric losses during petroleum production and processing that have large uncertainty and do not distinguish between gas that is flared as CO<sub>2</sub> or vented as CH<sub>4</sub>.  
 5 Fugitive emissions of CH<sub>4</sub> from the so-called upstream sector (e.g., coal mining and natural gas distribution) are not included in the accounts of CO<sub>2</sub> emissions except to the extent that they are captured in the UN energy data and counted as gas “flared or lost”.

The published CDIAC dataset has 250 countries and regions included. This expanded list includes countries that no longer exist, such as the USSR or East Pakistan. For the budget, we reduce the list to 216 countries by reallocating emissions to the currently defined territories. This involved both aggregation and disaggregation, and does not change global emissions. Examples of aggregation include merging East and West Germany to the currently defined Germany. Examples of disaggregation include real-  
 15 locating the emissions from former USSR to the resulting independent countries. For disaggregation, we use the emission shares when the current territory first appeared. For the most recent years, 2011–2013, the BP statistics are more aggregated, but we retain the detail of CDIAC by applying the growth rates of each aggregated region in the BP dataset to its constituent individual countries in CDIAC.

Estimates of CO<sub>2</sub> emissions show that the global total of emissions is not equal to the sum of emissions from all countries. This is largely attributable to emissions that occur in international territory, in particular the combustion of fuels used in international shipping and aviation (bunker fuels), where the emissions are included in the global totals but are not attributed to individual countries. In practice, the emissions  
 25 from international bunker fuels are calculated based on where the fuels were loaded, but they are not included with national emissions estimates. Other differences occur because globally the sum of imports in all countries is not equal to the sum of exports and because of differing treatment of oxidation of non-fuel uses of hydrocarbons (e.g. as solvents, lubricants, feedstocks, etc.), and changes in stock (Andres et al., 2012).

533

The uncertainty of the annual fossil fuel and cement emissions for the globe has been estimated at ±5% (scaled down from the published ±10% at ±2σ to the use of ±1σ bounds reported here; Andres et al., 2012). This is consistent with a more detailed recent analysis of uncertainty of ±8.4% at ±2σ (Andres et al., 2014). This includes  
 5 an assessment of uncertainties in the amounts of fuel consumed, the carbon and heat contents of fuels, and the combustion efficiency. While in the budget we consider a fixed uncertainty of ±5% for all years, in reality the uncertainty, as a percentage of the emissions, is growing with time because of the larger share of global emissions from non-Annex B countries (emerging economies and developing countries) with less precise statistical systems (Marland et al., 2009). For example, the uncertainty in Chinese emissions has been estimated at around ±10% (for ±1σ; Gregg et al., 2008). Generally, emissions from mature economies with good statistical bases have an uncertainty of only a few per cent (Marland, 2008). Further research is needed before we can quantify the time evolution of the uncertainty, and its temporal error correlation  
 15 structure. We note that even if they are presented as 1σ estimates, uncertainties of emissions are likely to be mainly country-specific systematic errors related to underlying biases of energy statistics and to the accounting method used by each country. We assign a medium confidence to the results presented here because they are based on indirect estimates of emissions using energy data (Durant et al., 2010). There is only limited and indirect evidence for emissions, although there is a high agreement among the available estimates within the given uncertainty (Andres et al., 2012, 2014), and emission estimates are consistent with a range of other observations (Ciais et al., 2013), even though their regional and national partitioning is more uncertain (Francey et al., 2013).

### 2.1.2 Emissions embodied in goods and services

National emission inventories take a territorial (production) perspective and “include greenhouse gas emissions and removals taking place within national territory and offshore areas over which the country has jurisdiction” (Rypdal et al., 2006). That is, emis-

534

sions are allocated to the country where and when the emissions actually occur. The territorial emission inventory of an individual country does not include the emissions from the production of goods and services produced in other countries (e.g. food and clothes) that are used for consumption. Consumption-based emission inventories for an individual country is another attribution point of view that allocates global emissions to products that are consumed within a country, and are conceptually calculated as the territorial emissions less the “embedded” territorial emissions to produce exported products plus the emissions in other countries to produce imported products (Consumption = Territorial – Exports + Imports). The difference between the territorial- and consumption-based emission inventories is the net transfer (exports minus imports) of emissions from the production of internationally traded products. Consumption-based emission attribution results (e.g. Davis and Caldeira, 2010) provide additional information to territorial-based emissions that can be used to understand emission drivers (Hertwich and Peters, 2009), quantify emission (virtual) transfers by the trade of products between countries (Peters et al., 2011b) and potentially design more effective and efficient climate policy (Peters and Hertwich, 2008).

We estimate consumption-based emissions by enumerating the global supply chain using a global model of the economic relationships between sectors within and between every country (Andrew and Peters, 2013; Peters et al., 2011a). Due to availability of the input data, detailed estimates are made for the years 1997, 2001, 2004, and 2007 (using the methodology of Peters et al., 2011b) using economic and trade data from the Global Trade and Analysis Project version 8.1 (GTAP; Narayanan et al., 2013). The results cover 57 sectors and 134 countries and regions. The results are extended into an annual time-series from 1990 to the latest year of the fossil fuel emissions or GDP data (2012 in this budget), using Gross Domestic Product (GDP) data by expenditure in current USD (from the UN National Accounts main Aggregates database; UN, 2014) and time series of trade data from GTAP (based on the methodology in Peters et al. 2011b).

535

The consumption-based emission inventories in this carbon budget incorporate several improvements over previous versions (Le Quéré et al., 2013; Peters et al., 2011b., 2012b). The detailed estimates for 2004 and 2007 and time series approximation from 1990–2012 are based on an updated version of the GTAP database (Narayanan et al., 2013). We estimate the sector-level CO<sub>2</sub> emissions using our own calculations based on the GTAP data and methodology, include flaring and cement emissions from CDIAC, and then scale the national totals (excluding bunker fuels) to match the CDIAC estimates from the most recent carbon budget. We do not include international transportation in our estimates of national totals, but include them in the global total. The time-series of trade data provided by GTAP covers the period 1995–2009 and our methodology uses the trade shares as this dataset. For the period 1990–1994 we assume the trade shares of 1995, while for 2010 and 2011 we assume the trade shares of 2008 since 2009 was heavily affected by the global financial crisis. We identified errors in the trade shares of Taiwan in 2008 and 2009, so its trade shares for 2008–2010 are based on the 2007 trade shares.

We do not provide an uncertainty estimate for these emissions, but based on model comparisons and sensitivity analysis, they are unlikely to be larger than for the territorial emission estimates (Peters et al., 2012a). Uncertainty is expected to increase for more detailed results, and to decrease with aggregation (Peters et al., 2011b; e.g. the results for Annex B will be more accurate than the sector results for an individual country).

The consumption-based emissions attribution method considers the CO<sub>2</sub> emitted to the atmosphere in the production of products, but not the trade in fossil fuels (coal, oil, gas). It is also possible to account for the carbon trade in fossil fuels (Davis et al., 2011), but we do not present that data here. Peters et al. (2012a) additionally considered trade in biomass.

The consumption data do not modify the global average terms in Eq. (1), but are relevant to the anthropogenic carbon cycle as they reflect the trade-driven movement of emissions across the Earth’s surface in response to human activities. Furthermore, if national and international climate policies continue to develop in an un-harmonised

536



## 2.2 CO<sub>2</sub> emissions from land use, land-use change and forestry ( $E_{LUC}$ )

LUC emissions reported in the 2014 carbon budget ( $E_{LUC}$ ) include CO<sub>2</sub> fluxes from deforestation, afforestation, logging (forest degradation and harvest activity), shifting cultivation (cycle of cutting forest for agriculture, then abandoning), and regrowth of forests following wood harvest or abandonment of agriculture. Only some land management activities (Table 5) are included in our LUC emissions estimates (e.g. emissions or sinks related to management and management changes of established pasture and croplands are not included). Some of these activities lead to emissions of CO<sub>2</sub> to the atmosphere, while others lead to CO<sub>2</sub> sinks.  $E_{LUC}$  is the net sum of all anthropogenic activities considered. Our annual estimate for 1959–2010 is from a bookkeeping method (Sect. 2.2.1) primarily based on net forest area change and biomass data from the Forest Resource Assessment (FRA) of the Food and Agriculture Organisation (FAO) which is only available at intervals of five years and ends in 2010 (Houghton et al., 2012). Inter-annual variability in emissions due to deforestation and degradation have been coarsely estimated from satellite-based fire activity in tropical forest areas (Sect. 2.2.2; Giglio, 2013; van der Werf et al., 2010). The bookkeeping method is used to quantify the  $E_{LUC}$  over the time period of the available data, and the satellite-based deforestation fire information to incorporate interannual variability ( $E_{LUC}$  flux annual anomalies) from tropical deforestation fires. The satellite-based deforestation and degradation fire emissions estimates are available for years 1997–2013. We calculate the global annual anomaly in deforestation and degradation fire emissions in tropical forest regions for each year, compared to the 1997–2010 period, and add this annual flux anomaly to the  $E_{LUC}$  estimated using the bookkeeping method that is available up to 2010 only and assumed constant at the 2010 value during the period 2011–2013. We thus assume that all land management activities apart from deforestation and degradation do not vary significantly on a year-to-year basis. Other sources of interannual variability (e.g. the impact of climate variability on regrowth fluxes and shifting agriculture CO<sub>2</sub> fluxes) are accounted for in  $S_{LAND}$ . In addition, we use results

539

from Dynamic Global Vegetation Models (see Sect. 2.2.3 and Table 6) that calculate net LUC CO<sub>2</sub> emissions in response to observed land cover change reconstructed from observations prescribed to each model, to help quantify the uncertainty in  $E_{LUC}$ , and to explore the consistency of our understanding. The three methods are described below, and differences are discussed in Sect. 3.2.

### 2.2.1 Bookkeeping method

LUC CO<sub>2</sub> emissions are calculated by a bookkeeping method approach (Houghton, 2003) that keeps track of the carbon stored in vegetation and soils before deforestation or other land-use change, and the changes in forest age classes, or cohorts, of disturbed lands after land-use change including possible forest regrowth after deforestation. It tracks the CO<sub>2</sub> emitted to the atmosphere immediately during deforestation, and over time due to the follow-up decay of soil and vegetation carbon in different pools, including wood products pools after logging and deforestation. It also tracks the regrowth of vegetation and associated build-up of soil carbon pools after LUC. It considers transitions between forests, pastures and cropland, shifting cultivation, degradation of forests where a fraction of the trees is removed, abandonment of agricultural land, and forest management such as wood harvest and, in the USA, fire management. In addition to tracking logging debris on the forest floor, the bookkeeping method tracks the fate of carbon contained in harvested wood products that is eventually emitted back to the atmosphere as CO<sub>2</sub>, although a detailed treatment of the lifetime in each product pool is not performed (Earles et al., 2012). Harvested wood products are partitioned into three pools with different turnover times. All fuel-wood is assumed burnt in the year of harvest (1.0 yr<sup>-1</sup>). Pulp and paper products are oxidized at a rate of 0.1 yr<sup>-1</sup>, timber is assumed to be oxidized at a rate of 0.01 yr<sup>-1</sup>, and elemental carbon decays at 0.001 yr<sup>-1</sup>. The general assumptions about partitioning wood products among these pools are based on national harvest data (Houghton, 2003).

The primary land cover change and biomass data for the bookkeeping method analysis is the Forest Resource Assessment of the FAO which provides statistics on forest

540

cover change and management at intervals of five years (FAO, 2010). The data is based on countries' self-reporting some of which include satellite data in more recent assessments (Table 4). Changes in land cover other than forest are based on annual, national changes in cropland and pasture areas reported by the FAO Statistics Division (FAOSTAT, 2010). LUC country data are aggregated by regions. The carbon stocks on land (biomass and soils), and their response functions subsequent to LUC, are based on FAO data averages per land cover type, per biome and per region. Similar results were obtained using forest biomass carbon density based on satellite data (Baccini et al., 2012). The bookkeeping method does not include land ecosystems' transient response to changes in climate, atmospheric CO<sub>2</sub> and other environmental factors, but the growth/decay curves are based on contemporary data that will implicitly reflect the effects of CO<sub>2</sub> and climate at that time. Results from the bookkeeping method are available from 1850 to 2010.

### 2.2.2 Fire-based method

LUC associated CO<sub>2</sub> emissions calculated from satellite-based fire activity in tropical forest areas (van der Werf et al., 2010) provide information on emissions due to tropical deforestation and degradation that are complementary to the bookkeeping approach. They do not provide a direct estimate of  $E_{LUC}$  as they do not include non-combustion processes such as respiration, wood harvest, wood products or forest regrowth. Legacy emissions such as decomposition from on-ground debris and soils are not included in this method either. However, fire estimates provide some insight in the year-to-year variations in the sub-component of the total  $E_{LUC}$  flux that result from immediate CO<sub>2</sub> emissions during deforestation caused, for example, by the interactions between climate and human activity (e.g. there is more burning and clearing of forests in dry years) that are not represented by other methods. The "deforestation fire emissions" assume an important role of fire in removing biomass in the deforestation process, and thus can be used to infer gross instantaneous CO<sub>2</sub> emissions from deforestation using satellite-derived data on fire activity in regions with active deforestation. The method

541

requires information on the fraction of total area burned associated with deforestation versus other types of fires, and can be merged with information on biomass stocks and the fraction of the biomass lost in a deforestation fire to estimate CO<sub>2</sub> emissions. The satellite-based deforestation fire emissions are limited to the tropics, where fires result mainly from human activities. Tropical deforestation is the largest and most variable single contributor to  $E_{LUC}$ .

*Fire emissions associated with deforestation and tropical peat burning are based on the Global Fire Emissions Database (GFED) described in van der Werf et al. (2010) but with updated burned area (Giglio, 2013) as well as burned area from relatively small fires that are detected by satellite as thermal anomalies but not mapped by the burned area approach (Randerson, 2012).* The burned area information is used as input data in a modified version of the satellite-driven Carnegie Ames Stanford Approach (CASA) biogeochemical model to estimate carbon emissions associated with fires, keeping track of what fraction of fire emissions was due to deforestation (see van der Werf et al., 2010). The CASA model uses different assumptions to compute decay functions compared to the bookkeeping method, and does not include historical emissions or regrowth from land-use change prior to the availability of satellite data. Comparing coincident CO emissions and their atmospheric fate with satellite-derived CO concentrations allows for some validation of this approach (e.g. van der Werf et al., 2008). Results from the fire-based method to estimate LUC emissions anomalies added to the bookkeeping mean  $E_{LUC}$  estimate are available from 1997 to 2013. Our combination of LUC CO<sub>2</sub> emissions where the variability of annual CO<sub>2</sub> deforestation emissions is diagnosed from fires assumes that year-to-year variability is dominated by variability in deforestation.

### 2.2.3 Dynamic Global Vegetation Models (DGVMs)

LUC CO<sub>2</sub> emissions have been estimated using an ensemble of seven DGVMs (from nine in the 2012 carbon budget). New model experiments up to year 2013 have been coordinated by the project "Trends and drivers of the regional-scale sources and sinks

542

of carbon dioxide (TRENDY; <http://dgvn.ceh.ac.uk/node/9>)". We use only models that have estimated LUC CO<sub>2</sub> emissions and the terrestrial residual sink following the TRENDY protocol (see Sect. 2.5.2), thus providing better consistency in the assessment of the causes of carbon fluxes on land. Models use their latest configurations, summarised in Tables 5 and 6.

The DGVMs were forced with historical changes in land cover distribution, climate, atmospheric CO<sub>2</sub> concentration, and N deposition. As further described below, each historical DGVM simulation was repeated with a time-invariant pre-industrial land cover distribution, allowing to estimate, by difference with the first simulation, the dynamic evolution of biomass and soil carbon pools in response to prescribed land cover change. All DGVMs represent deforestation and (to some extent) regrowth, the most important components of  $E_{LUC}$ , but they do not represent all processes resulting directly from human activities on land (Table 5). DGVMs represent processes of vegetation growth, mortality and decomposition associated with natural cycles and include the vegetation and soil response to increasing atmospheric CO<sub>2</sub> levels, to climate variability and change, in addition to atmospheric N deposition in the presence of nitrogen limitation (in four models; Table 5). The DGVMs are independent from the other budget terms except for their use of atmospheric CO<sub>2</sub> concentration to calculate the fertilization effect of CO<sub>2</sub> on primary production.

The DGVMs used a consistent land-use change dataset (Hurtt et al., 2011), which provided annual, half-degree, fractional data on cropland, pasture, primary vegetation and secondary vegetation, as well as all underlying transitions between land-use states, including wood harvest and shifting cultivation. This dataset used the HYDE (Klein Goldewijk et al., 2011) spatially gridded maps of cropland, pasture, and ice/water fractions of each grid cell as an input. The HYDE data is based on annual FAO statistics of change in agricultural area (FAOSTAT, 2010). *For the years 2011, 2012 and 2013*, the HYDE dataset was extrapolated by country for pastures and cropland separately based on the trend in agricultural area over the previous 5 years. The HYDE dataset is independent from the data set used in the bookkeeping method (Houghton, 2003

and updates), which is based primarily on forest area change statistics (FAO, 2010). Although the Hurtt land-use change dataset indicates whether land-use changes occur on forested or non-forested land, typically only the changes in agricultural areas are used by the models and are implemented differently within each model (e.g. an increased cropland fraction in a grid cell can either be at the expense of grassland, or forest, the latter resulting in deforestation; land cover fractions of the non-agricultural land differ between models). Thus the DGVM forest area and forest area change over time is not consistent with the Forest Resource Assessment of the FAO forest area data used for the book-keeping model to calculate  $E_{LUC}$ . Similarly, model-specific assumptions are also applied for the conversion of wood harvest mass or area and other product pools into carbon in some models (Table 5).

The DGVM model runs were forced by either 6 hourly CRU-NCEP or by monthly temperature, precipitation, and cloud cover fields (transformed into incoming surface radiation) based on observations and provided on a 0.5° × 0.5° grid and updated to 2013 (CRU TS3.22; Harris et al., 2014). The forcing data include both gridded observations of climate change and change in global atmospheric CO<sub>2</sub> (Dlugokencky and Tans, 2014), and N deposition (as used in 4 models, Table 5; Lamarque et al., 2010).  $E_{LUC}$  is diagnosed in each model by the difference between a model simulation with prescribed historical land cover change and a simulation with constant, pre-industrial land cover distribution. Both simulations were driven by changing atmospheric CO<sub>2</sub>, climate, and in some models N deposition over the period 1860–2013. Using the difference between these two DGVM simulations to diagnose  $E_{LUC}$  is not consistent with the definition of  $E_{LUC}$  in the bookkeeping method (Gasser and Ciais, 2013; Pongratz et al., 2013). The DGVM approach to diagnose land-use change CO<sub>2</sub> emissions is expected to produce systematically higher  $E_{LUC}$  emissions than the bookkeeping approach if all the parameters of the two approaches were the same (which is not the case). Here, given the different input data of DGVMs and the bookkeeping approach, this systematic difference cannot be quantified.

## 2.2.4 Uncertainty assessment for $E_{LUC}$

Differences between the bookkeeping, the addition of fire-based interannual variability to the bookkeeping, and DGVM methods originate from three main sources: the land cover change data set, different approaches in models, and in the different processes represented (Table 5). We examine the results from the seven DGVM models and of the bookkeeping method to assess the uncertainty in  $E_{LUC}$ .

The uncertainties in the annual  $E_{LUC}$  estimates are examined using the standard deviation across models, which ranged from 0.3 to 1.1 GtC yr<sup>-1</sup>, with an average of 0.7 GtC yr<sup>-1</sup> from 1959 to 2013 (Table 7). The mean of the multi-model  $E_{LUC}$  estimates is the same as the mean of the bookkeeping estimate from the budget (Eq. 1) at 1.3 GtC for 1959 to 2010. The multi-model mean and bookkeeping method differ by less than 0.5 GtC yr<sup>-1</sup> over 90 % of the time. Based on this comparison, we assess that an uncertainty of  $\pm 0.5$  GtC yr<sup>-1</sup> provides a semi-quantitative measure of uncertainty for annual emissions, and reflects our best value judgment that there is at least 68 % chance ( $\pm 1\sigma$ ) that the true LUC emission lies within the given range, for the range of processes considered here. This is consistent with the analysis of Houghton et al. (2012), which partly reflects improvements in data on forest area change using satellite data, and partly more complete understanding and representation of processes in models.

The uncertainties in the decadal mean estimates from the DGVM ensemble are likely correlated between decades, and thus we apply the annual uncertainty as a measure of the decadal uncertainty. The correlations between decades come from (1) common biases in system boundaries (e.g. not counting forest degradation in some models); (2) common definition for the calculation of  $E_{LUC}$  from the difference of simulations with and without LUC (a source of bias vs. the unknown truth); (3) common and uncertain land-cover change input data which also cause a bias, though if a different input dataset is used each decade, decadal fluxes from DGVMs may be partly decorrelated; (4) model structural errors (e.g. systematic errors in biomass stocks). In addition, errors arising from uncertain DGVM parameter values would be random but they are not ac-

545

counted for in this study, since no DGVM provided an ensemble of runs with perturbed parameters.

Prior to 1959, the uncertainty in  $E_{LUC}$  is taken as  $\pm 33\%$ , which is the ratio of uncertainty to mean from the 1960s (Table 7), the first decade available. This ratio is consistent with the mean standard deviation of DGVMs LUC emissions over 1870–1958 (0.41 GtC) over the multi-model mean (0.94 GtC).

## 2.3 Atmospheric CO<sub>2</sub> growth rate ( $G_{ATM}$ )

### 2.3.1 Global atmospheric CO<sub>2</sub> growth rate estimates

The atmospheric CO<sub>2</sub> growth rate is provided by the US National Oceanic and Atmospheric Administration Earth System Research Laboratory (NOAA/ESRL; Dlugokencky and Tans, 2014), which is updated from Ballantyne et al. (2012). For the 1959–1980 period, the global growth rate is based on measurements of atmospheric CO<sub>2</sub> concentration averaged from the Mauna Loa and South Pole stations, as observed by the CO<sub>2</sub> Program at Scripps Institution of Oceanography (Keeling et al., 1976). For the 1980–2012 time period, the global growth rate is based on the average of multiple stations selected from the marine boundary layer sites with well-mixed background air (Ballantyne et al., 2012), after fitting each station with a smoothed curve as a function of time, and averaging by latitude band (Masarie and Tans, 1995). The annual growth rate is estimated by Dlugokencky and Tans (2014) from atmospheric CO<sub>2</sub> concentration by taking the average of the most recent December-January months corrected for the average seasonal cycle and subtracting this same average one year earlier. The growth rate in units of ppm yr<sup>-1</sup> is converted to fluxes by multiplying by a factor of 2.120 GtC per ppm (Prather et al., 2012) for comparison with the other components.

The uncertainty around the annual growth rate based on the multiple stations dataset ranges between 0.11 and 0.72 GtC yr<sup>-1</sup>, with a mean of 0.60 GtC yr<sup>-1</sup> for 1959–1980 and 0.19 GtC yr<sup>-1</sup> for 1980–2013, when a larger set of stations were available (Dlugokencky and Tans, 2014). It is based on the number of available stations, and thus takes

546





### 2.4.3 Uncertainty assessment for $S_{\text{OCEAN}}$

The uncertainty around the mean ocean sink of anthropogenic  $\text{CO}_2$  was already quantified for the 1990s (see Sect. 2.4.1). To quantify the uncertainty around annual values, we examine the standard deviation of the normalised model ensemble. We use further information from the three data-based products to assess the confidence level. The standard deviation of the ocean model ensemble averages to  $0.15 \text{ GtC yr}^{-1}$  during 1980–2010 (with a maximum of 0.22), but it increases as the model ensemble goes back in time, with a standard deviation of  $0.28 \text{ GtC yr}^{-1}$  across models in the 1960s. We estimate that the uncertainty in the annual ocean  $\text{CO}_2$  sink is about  $\pm 0.5 \text{ GtC yr}^{-1}$  from the fractional uncertainty of the data uncertainty of  $\pm 0.4 \text{ GtC yr}^{-1}$  and standard deviation across models of up to  $\pm 0.28 \text{ GtC yr}^{-1}$ , reflecting both the uncertainty in the mean sink from observations during the 1990's (Denman et al., 2007; Sect. 2.4.1) and in the interannual variability as assessed by models.

We examine the consistency between the variability of the model-based and the data-based products to assess confidence in  $S_{\text{OCEAN}}$ . The interannual variability of the ocean fluxes (quantified as the standard deviation) of the three data-based estimates for 1990–2009 (when they overlap) is  $\pm 0.37 \text{ GtC yr}^{-1}$  (Rödenbeck et al., 2014),  $\pm 0.25 \text{ GtC yr}^{-1}$  (Landschützer et al., 2014), and  $\pm 0.14 \text{ GtC yr}^{-1}$  (Park et al., 2010), compared to  $\pm 0.18 \text{ GtC yr}^{-1}$  for the model mean. The standard deviation includes a component of trend and decadal variability in addition to interannual variability, and their relative influence differs across estimates. The phase is generally consistent between estimates, with a higher ocean  $\text{CO}_2$  sink during El Niño events. The annual data-based estimates correlate with the ocean  $\text{CO}_2$  sink estimated here with a correlation of  $r = 0.36$  (0.0 to 0.49 for individual models),  $r = 0.73$  (0.54 to 0.68), and  $r = 0.64$  (0.12 to 0.71) for the data-based estimates of Rödenbeck et al. (2014), Landschützer et al. (2014), and Park et al. (2010), respectively (simple linear regression), but their mutual correlation ranges between 0.24 and 0.31 only. The use of annual data for the correlation may reduce the correlation because the dominant source of variability asso-

551

ciated with El Niño events is less than one year. We assess a medium confidence level to the annual ocean  $\text{CO}_2$  sink and its uncertainty because they are based on multiple lines of evidence, and *the results are consistent in that the interannual variability in the model and data-based estimates are all generally small compared to the variability in atmospheric  $\text{CO}_2$  growth rate. Nevertheless the various results do not show high agreement in amplitude on the global scale and for the relative roles of the annual and decadal variability compared to the trend.*

### 2.5 Terrestrial $\text{CO}_2$ sink

The difference between the fossil fuel ( $E_{\text{FF}}$ ) and LUC net emissions ( $E_{\text{LUC}}$ ), the growth rate in atmospheric  $\text{CO}_2$  concentration ( $G_{\text{ATM}}$ ) and the ocean  $\text{CO}_2$  sink ( $S_{\text{OCEAN}}$ ) is attributable to the net sink of  $\text{CO}_2$  in terrestrial vegetation and soils ( $S_{\text{LAND}}$ ), within the given uncertainties. Thus, this sink can be estimated either as the residual of the other terms in the mass balance budget but also directly calculated using DGVMs or estimated from inverse models that close a spatiotemporally explicit form of the mass balance in Eq. (1). The residual land sink ( $S_{\text{LAND}}$ ) is thought to be in part because of the fertilising effect of rising atmospheric  $\text{CO}_2$  on plant growth, N deposition and climate change effects such as the lengthening of the growing season in northern temperate and boreal areas.  $S_{\text{LAND}}$  does not include gross land sinks directly resulting from LUC (e.g. regrowth of vegetation) as these are estimated as part of the net land use flux ( $E_{\text{LUC}}$ ). System boundaries make it difficult to attribute exactly  $\text{CO}_2$  fluxes on land between  $S_{\text{LAND}}$  and  $E_{\text{LUC}}$  (Erb et al., 2013), and by design most of the uncertainties in our method are allocated to  $S_{\text{LAND}}$  for those processes that are poorly known or represented in models.

552

### 2.5.1 Residual of the budget

For 1959–2013, the terrestrial carbon sink was estimated from the residual of the other budget terms by rearranging Eq. (1):

$$S_{\text{LAND}} = E_{\text{FF}} + E_{\text{LUC}} - (G_{\text{ATM}} + S_{\text{OCEAN}}) \quad (8)$$

- 5 The uncertainty in  $S_{\text{LAND}}$  is estimated annually from the root sum of squares of the uncertainty in the right-hand terms assuming the errors are not correlated. The uncertainty averages to  $\pm 0.8 \text{ GtC yr}^{-1}$  over 1959–2013 (Table 7).  $S_{\text{LAND}}$  estimated from the residual of the budget includes, by definition, all the missing processes and potential biases in the other components of Eq. (8).

### 10 2.5.2 DGVMs

A comparison of the residual calculation of  $S_{\text{LAND}}$  in Eq. (8) with estimates from DGVMs as used to estimate  $E_{\text{LUC}}$  in Sect. 2.2.3, but here excluding the effects of changes in land cover (using a constant pre-industrial land cover distribution), provides an independent estimate of the consistency of  $S_{\text{LAND}}$  with our understanding of the functioning of the terrestrial vegetation in response to  $\text{CO}_2$  and climate variability (Table 7). As described in Sect. 2.2.3, the DGVM runs that exclude the effects of changes in land cover include all climate variability and  $\text{CO}_2$  effects over land, but do not include reductions in  $\text{CO}_2$  sink capacity associated with human activity directly affecting changes in vegetation cover and management, which by design is allocated to  $E_{\text{LUC}}$ . This effect has been estimated to have led to a reduction in the terrestrial sink by  $0.5 \text{ GtC yr}^{-1}$  since 1750 (Gitz and Ciais, 2003). The models in this configuration estimate the mean and variability of  $S_{\text{LAND}}$  based on atmospheric  $\text{CO}_2$  and climate, and thus both terms can be compared to the budget residual.

The multi-DGVM mean of  $2.5 \pm 1.0 \text{ GtC yr}^{-1}$  for the period 2004–2013 agrees well with the value computed from the budget residual (Table 7). The standard deviation of the annual  $\text{CO}_2$  sink across the nine DGVMs ranges from  $\pm 0.4$  to  $\pm 1.4 \text{ GtC yr}^{-1}$ , with a

553

mean standard deviation of  $\pm 0.9 \text{ GtC yr}^{-1}$  for the period 1959 to 2013. The model mean correlates with the budget residual with  $r = 0.71$ , compared to correlations of  $r = 0.46$  to  $r = 0.70$  (median of 0.61) between individual models. The standard deviation is similar to that of the five model ensembles presented in Le Quéré et al. (2009), but the correlation is improved compared to  $r = 0.54$  obtained in the earlier study. The DGVM results suggest that the sum of our knowledge on annual  $\text{CO}_2$  emissions and their partitioning is plausible (see Discussion), and provide insight on the underlying processes and regional breakdown. However as the standard deviation across the DGVMs (of  $\pm 0.9 \text{ GtC yr}^{-1}$ ) is of the same magnitude as the combined uncertainty due to the other components ( $E_{\text{FF}}$ ,  $E_{\text{LUC}}$ ,  $G_{\text{ATM}}$ ,  $S_{\text{OCEAN}}$ ; Table 7), the DGVMs do not provide further reduction of uncertainty on the terrestrial  $\text{CO}_2$  sink compared to the residual of the budget (Eq. 8). Yet, DGVM results are largely independent from the residual of the budget, and it is worth noting that the residual method and ensemble mean DGVM results are consistent within their respective uncertainties. We assess a medium confidence level to the annual land  $\text{CO}_2$  sink and its uncertainty because the estimates from the residual budget and averaged DGVMs match well within their respective uncertainties, and the estimates based on the residual budget are primarily dependent on  $E_{\text{FF}}$  and  $G_{\text{ATM}}$ , both of which are well constrained.

### 2.6 View from the atmosphere

20 *The world-wide network of atmospheric measurements can be used with atmospheric inversion methods to constrain the location of the combined surface  $\text{CO}_2$  fluxes from all sources, including fossil and LUC emissions and land and ocean  $\text{CO}_2$  sinks. As the geographical distribution of fossil fuel emissions is already known, it can be removed from the signal to provide a view from the atmosphere of the  $\text{CO}_2$  fluxes over land and over the ocean. Here we used preliminary atmospheric  $\text{CO}_2$  data to the end of 2013, and three atmospheric  $\text{CO}_2$  inversions (Table 6) to infer the total  $\text{CO}_2$  flux over land regions, and the distribution of the total land + ocean  $\text{CO}_2$  fluxes for the North, Tropics*

and South. We focus here on the largest and most consistent sources of information, and use these estimates to comment on the consistency across various data streams and process-based estimates.

### 2.6.1 Atmospheric inversions

5 The three inversion systems used in this release (Chevallier, 2005; Peters, 2010; Rödenbeck, 2005) are based on the same Bayesian inversion principles and interpret mostly the same observed time series (or subsets thereof), but use different methodologies that represent a cross-cut of the many approaches used in the field. This concerns the time resolution of the estimates (weekly, monthly), their spatial breakdown  
10 (grid size), their assumed correlation structures, and the mathematical approach (4d-VAR, EnKF). The details of these approaches are documented extensively in the references provided. Most importantly, each system has used a different atmospheric transport model, which was demonstrated to be a driving factor behind differences in atmospheric-based flux estimates, and specifically their global distribution (Stephens et al., 2007). Most inverse models use prior estimates for the ocean and land-biosphere,  
15 sometimes very similar to those used in Sects. 2.4.1 and 2.5.1 above to assign prior fluxes. They do not separately estimate  $E_{FF}$  but rather use similar data sources as described in Sects. 2.1.1, and 2.2.2 above to set these. Finally atmospheric inversions include  $CO_2$  fluxes from rivers (which need to be taken into account in the comparison  
20 to the other information sources), and chemical oxidation of reactive carbon-containing gases (which are neglected here). These inverse estimates are not truly independent of the other estimates presented here because the atmospheric observations encompass the set of atmospheric observations used for the global growth rate (Sect. 2.3). However they provide new information on the regional distribution of the fluxes.

25 In this first carbon budget release including inverse models we focus the analysis on two known strengths of the inverse approach: the derivation of year-to-year changes in total land ( $E_{LUC} + S_{LAND}$ ) fluxes consistent with the whole network of atmospheric observations, and the spatial breakdown of land and ocean fluxes ( $E_{LUC} + S_{LAND} + S_{OCEAN}$ )

555

across large regions of the globe. The total land flux correlate well with those estimated from the budget residual (Eq. 1) with correlations ranging from  $r = 0.84$  to  $0.93$ , and with the DGVM multi-model mean with correlations ranging from  $r = 0.71$  to  $0.84$  ( $r = 0.37$  to  $0.82$  for individual DGVMs and inversions). The spatial breakdown is discussed in  
5 Sect. 3.1.3.

## 2.7 Processes not included in the global carbon budget

### 2.7.1 Contribution of anthropogenic CO and CH<sub>4</sub> to the global carbon budget

Anthropogenic emissions of CO and CH<sub>4</sub> to the atmosphere are eventually oxidized to CO<sub>2</sub> and thus are part of the global carbon budget. These contributions are omitted in  
10 Eq. (1), but an attempt is made in this section to estimate their magnitude, and identify the sources of uncertainty. Anthropogenic CO emissions are from incomplete fossil fuel and biofuel burning and deforestation fires. The main anthropogenic emissions of fossil CH<sub>4</sub> that matter for the global carbon budget are the fugitive emissions of coal, oil and gas upstream sectors (see below). These emissions of CO and CH<sub>4</sub> contribute a net  
15 addition of fossil carbon to the atmosphere.

In our estimate of  $E_{FF}$  we assumed (Sect. 2.1.1) that all the fuel burned is emitted as CO<sub>2</sub>, thus CO anthropogenic emissions and their atmospheric oxidation into CO<sub>2</sub> within a few months are already counted implicitly in  $E_{FF}$  and should not be counted twice (same for  $E_{LUC}$  and anthropogenic CO emissions by deforestation fires). Anthropogenic emissions of fossil CH<sub>4</sub> are not included in  $E_{FF}$ , because these fugitive  
20 emissions are not included in the fuel inventories. Yet they contribute to the annual CO<sub>2</sub> growth rate after CH<sub>4</sub> gets oxidized into CO<sub>2</sub>. Anthropogenic emissions of fossil CH<sub>4</sub> represent 15 % of total CH<sub>4</sub> emissions (Kirschke et al., 2013) that is  $61 \text{ Tg C yr}^{-1}$  for the past decade. Assuming steady state, these emissions are all converted to CO<sub>2</sub>  
25 by OH oxidation, and thus explain  $0.06 \text{ PgC yr}^{-1}$  of the global CO<sub>2</sub> growth rate in the past decade.

556

Other anthropogenic changes in the sources of CO and CH<sub>4</sub> from wildfires, biomass, wetlands, ruminants or permafrost changes are similarly assumed to have a small effect on the CO<sub>2</sub> growth rate.

## 2.7.2 Anthropogenic carbon fluxes in the land to ocean continuum

5 The approach used to determine the global carbon budget considers only anthropogenic CO<sub>2</sub> emissions and their partitioning among the atmosphere, ocean and land. In this analysis, the land and ocean reservoirs that take up anthropogenic CO<sub>2</sub> from the atmosphere are conceived as independent carbon storage repositories. This approach thus omits that carbon is continuously displaced along the land-ocean aquatic continuum (LOAC) comprising freshwaters, estuaries and coastal areas. Carbon is transferred both in inorganic (bicarbonates and dissolved CO<sub>2</sub>), and organic (dissolved and particulate organic carbon) forms along this continuum (Bauer et al., 2013). During its journey from upland terrestrial ecosystems to the oceans, carbon is not only transferred laterally, but is also sequestered in e.g. freshwater and coastal sediments (Krumins et al., 2013; Tranvik et al., 2009) or released back to the atmosphere, mainly as respired CO<sub>2</sub> (Aufdenkampe et al., 2011; Battin et al., 2009; Cole et al., 2007; Laruelle et al., 2010; Regnier et al., 2013), and to a much lesser extent, as CH<sub>4</sub> (Bastviken et al., 2011; Borges and Abril, 2011). A significant fraction of this lateral carbon flux is entirely “natural” and is thus a steady state component of the pre-industrial carbon cycle that can be ignored in the current analysis. The remaining fraction is anthropogenic carbon entrained into the lateral transport loop of the LOAC, a perturbation that is relevant for the global carbon budget presented here.

The recent synthesis by Regnier et al. (2013) is the first attempt to estimate the anthropogenic component of LOAC carbon fluxes and their significance for the global carbon budget. The results of their analysis can be summarized in three points of relevance to the budget. First, only a portion of the anthropogenic CO<sub>2</sub> taken up by land ecosystems is sequestered in soil and biomass pools, as  $1 \pm 0.5 \text{ GtC yr}^{-1}$  is exported to the LOAC. This flux is comparable to the C released to the atmosphere by LUC (Ta-

557

ble 8). Second, the exported anthropogenic carbon is both stored ( $0.55 \pm 0.3 \text{ GtC yr}^{-1}$ ) and released back to the atmosphere as CO<sub>2</sub> ( $0.35 \pm 0.2 \text{ GtC yr}^{-1}$ ), the magnitude of these fluxes resulting from the combined effects of freshwaters, estuaries and coastal seas. Third, a small fraction of anthropogenic carbon displaced by the LOAC accumulates in the open ocean ( $0.1 \pm > 0.05 \text{ GtC yr}^{-1}$ ). The anthropogenic perturbation of the carbon fluxes from land to ocean does not contradict the method used in Sect. 2.5 to define the ocean sink and residual land sink. However, it does point to the need to account for the fate of anthropogenic carbon once it is removed from the atmosphere by land ecosystems (summarized in Fig. 2). In theory, direct estimates of changes of the ocean inorganic carbon inventory over time would see the land flux of anthropogenic carbon and would thus have a bias relative to air-sea flux estimates and tracer based reconstructions. However, currently the value is small enough to be not noticeable relative to the errors in the individual techniques.

More importantly the residual land sink (here land being terrestrial ecosystems) calculated in a budget which accounts for the LOAC ( $3.25 \pm 0.9 \text{ GtC yr}^{-1}$ ) is larger than the residual land sink ( $S_{\text{LAND}}$ ) value of  $2.85 \pm 0.8 \text{ GtC yr}^{-1}$  (2004–2013) reported in Table 8. This is because this flux is partially offset by a net source of CO<sub>2</sub> to the atmosphere of  $0.35 \pm 0.3 \text{ GtC yr}^{-1}$  from rivers, estuaries and coastal seas. In addition, because anthropogenic CO<sub>2</sub> taken up by land ecosystems is exported to the LOAC, the annual land carbon storage change ( $1.35 \text{ GtC yr}^{-1}$ ) is notably smaller than the residual uptake by land ecosystems ( $S_{\text{LAND}}$ ) calculated in the GCP budget ( $2.9 \text{ GtC yr}^{-1}$ ), a significant fraction of the displaced carbon ( $0.65 \text{ GtC yr}^{-1}$ ) from land ecosystems that is stored in freshwater and coastal sediments ( $0.55 \text{ GtC yr}^{-1}$ ), and to a lesser extent, in the open ocean ( $0.1 \text{ GtC yr}^{-1}$ ).

All estimates of LOAC are given with low confidence, because they originate from a single source. The carbon budget presented here implicitly incorporates the fluxes from the LOAC with  $S_{\text{LAND}}$ . We do not attempt to separate these fluxes because the uncertainties in either estimate are too large, and there is insufficient information available to estimate the LOAC fluxes on an annual basis.

### 3 Results

#### 3.1 Global carbon budget averaged over decades and its variability

The global carbon budget averaged over the last decade (2004–2013) is shown in Fig. 2. For this time period, 91 % of the total emissions ( $E_{\text{FF}} + E_{\text{LUC}}$ ) were caused by fossil fuel combustion and cement production, and 9 % by land-use change. The total emissions were partitioned among the atmosphere (44 %), ocean (26 %) and land (29 %). All components except land-use change emissions have grown since 1959 (Figs. 3 and 4), with important interannual variability in the atmospheric growth rate and in the land  $\text{CO}_2$  sink (Fig. 4), and some decadal variability in all terms (Table 8).

##### 3.1.1 $\text{CO}_2$ emissions

Global  $\text{CO}_2$  emissions from fossil fuel combustion and cement production have increased every decade from an average of  $3.1 \pm 0.2 \text{ GtC yr}^{-1}$  in the 1960s to an average of  $8.9 \pm 0.4 \text{ GtC yr}^{-1}$  during 2004–2013 (Table 8 and Fig. 5). The growth rate in these emissions decreased between the 1960s and the 1990s, from  $4.5 \% \text{ yr}^{-1}$  in the 1960s (1960–1969),  $2.9 \% \text{ yr}^{-1}$  in the 1970s (1970–1979),  $1.9 \% \text{ yr}^{-1}$  in the 1980s (1980–1989),  $1.0 \% \text{ yr}^{-1}$  in the 1990s (1990–1999), and began increasing again in the 2000s at an average growth rate of  $3.3 \% \text{ yr}^{-1}$ , decreasing slightly, to  $2.5 \% \text{ yr}^{-1}$  for the last decade (2004–2013). In contrast,  $\text{CO}_2$  emissions from LUC have remained constant at around  $1.5 \pm 0.5 \text{ GtC yr}^{-1}$  between 1960–1999, and decreased to  $0.9 \pm 0.5 \text{ GtC yr}^{-1}$  during 2004–2013. The  $E_{\text{LUC}}$  estimates from the bookkeeping method and the DGVM models are consistent within their respective uncertainties (Table 7 and Fig. 6). The decrease in emissions from LUC since 2000 is reproduced by the DGVMs (Fig. 6).

559

##### 3.1.2 Partitioning

The growth rate in atmospheric  $\text{CO}_2$  increased from  $1.7 \pm 0.1 \text{ GtC yr}^{-1}$  in the 1960s to  $4.3 \pm 0.1 \text{ GtC yr}^{-1}$  during 2004–2013 with important decadal variations (Table 8). Both ocean and land  $\text{CO}_2$  sinks increased roughly in line with the atmospheric increase, but with significant decadal variability on land (Table 8). The ocean  $\text{CO}_2$  sink increased from  $1.1 \pm 0.5 \text{ GtC yr}^{-1}$  in the 1960s to  $2.6 \pm 0.5 \text{ GtC yr}^{-1}$  during 2004–2013, with interannual variations of the order of a few tenths of  $\text{GtC yr}^{-1}$  generally showing an increased ocean sink during El Niño events (Fig. 7). Although there is some coherence between the ocean models and data products and among data products, their mutual correlation is weak and highlight disagreement on the exact amplitude of the interannual variability, and on the relative importance of the trend versus the variability (Sect. 2.4.3 and Fig. 7). Most estimates produce a mean  $\text{CO}_2$  sink for the 1990s that is below the mean assessed by the IPCC from indirect (but arguably more reliable) observations (Sect. 2.4.1). This could reflect issues with the vertical diffusion in ocean models, though as data-products also support a lower mean  $\text{CO}_2$  sink, this may also suggest a need to reassess the mean carbon sinks.

The land  $\text{CO}_2$  sink increased from  $1.8 \pm 0.7 \text{ GtC yr}^{-1}$  in the 1960s to  $2.9 \pm 0.8 \text{ GtC yr}^{-1}$  during 2004–2013, with important interannual variations of up to  $2 \text{ GtC yr}^{-1}$  generally showing a decreased land sink during El Niño events, overcompensating the increased in ocean sink and accounting for the enhanced atmospheric growth rate during El Niño events (Poulter et al., 2014). The high uptake anomaly around year 1991 is thought to be caused by the effect of the volcanic eruption of Mount Pinatubo on climate (Mercado et al., 2009) and is not generally reproduced by the DGVMs but assigned to  $S_{\text{LAND}}$  by the two inverse systems that include this period (Fig. 6). The larger land  $\text{CO}_2$  sink during 2004–2013 compared to the 1960s is reproduced by all the DGVMs in response to combined atmospheric  $\text{CO}_2$  increase and climate change and variability (average change of  $1.4 \text{ GtC yr}^{-1}$ ; eight models ranging between  $0.8$  and  $2.3 \text{ GtC yr}^{-1}$  with one model at  $0.1 \text{ GtC yr}^{-1}$ ), consistent with the

560

budget residual and reflecting a common knowledge of the processes (Table 7). The decadal change is also consistent with the results from the atmospheric inversions who estimate a trend of 0.84 and 0.62 GtC yr<sup>-1</sup> per decade, for the inversions of Chevallier et al. (2005) and Rödenbeck et al. (2003), respectively.

5 The total CO<sub>2</sub> fluxes on land ( $E_{\text{LUC}} + S_{\text{LAND}}$ ) constrained by the atmospheric inversions show in general very good agreement with the global budget estimate, as expected given the strong constraint of  $G_{\text{ATM}}$  and the small relative uncertainty typically assumed on  $S_{\text{OCEAN}}$  and  $E_{\text{FF}}$  by inversions. The total sink is of similar magnitude for the decadal average, with estimates from the inversions of 1.7, 2.0 and 3.1 GtC yr<sup>-1</sup> compared 10  $2.0 \pm 0.6$  GtC yr<sup>-1</sup> for the budget residual (Tables 7). The inversions' total land sink would be 1.2, 1.5, and 2.6 GtC yr<sup>-1</sup> when including a mean river flux correction of 0.45 GtC yr<sup>-1</sup>, though the exact correction would be smaller when taking into account the anthropogenic contribution to river fluxes (Sect. 2.7.2). The IAV of the inversions also matches the residual-based  $S_{\text{LAND}}$  closely (Fig. 6). The multi-model mean from 15 the DGVM ensemble that performed LUC simulations also compare well with the estimate from the residual budget and atmospheric inversions, with a decadal mean of  $1.4 \pm 0.9$  GtC yr<sup>-1</sup> (Table 7), although individual models differ by several GtC for some years (Fig. 6).

### 3.1.3 Distribution

20 The total surface CO<sub>2</sub> fluxes on land and ocean including LUC ( $E_{\text{LUC}} + S_{\text{LAND}} + S_{\text{OCEAN}}$ ) distributed regionally by latitude band according to atmospheric inversions show some consistency across regions and methods. In the South (south of 30° S), the atmospheric inversions and combined models all suggest a CO<sub>2</sub> sink between 1.3 and 1.6 GtC yr<sup>-1</sup>, increasing with time (Fig. 8), although the details of the interannual variability are not consistent across methods. The interannual variability in the South is low 25 because of the dominance of ocean area with low variability compared to land areas. In the tropics (30° S–30° N), both the atmospheric inversions and combined models

561

suggest the carbon balance in this region is close to neutral over the past decade. It is also the source of the largest variability, both at the interannual time scale but also with large decadal variability. Finally in the North (north of 30° N), the inversions and combined models disagree on the magnitude of the CO<sub>2</sub> sink with the ensemble 5 mean of the process models suggesting a smaller total Northern Hemisphere sink of  $2.1 \pm 0.6$  GtC yr<sup>-1</sup> while the inversions estimate a sink of between 2.4 and 3.5 GtC yr<sup>-1</sup>, though some agreement exists in the IAV. The mean difference cannot be explained by the influence of river fluxes alone, as the river fluxes in the Northern Hemisphere would be less than 0.45 GtC yr<sup>-1</sup>, particularly when taking into account for the anthropogenic 10 contribution to river fluxes.

## 3.2 Global carbon budget for year 2013 and emissions projection for 2014

### 3.2.1 CO<sub>2</sub> emissions

Global CO<sub>2</sub> emissions from fossil fuel combustion and cement production reached  $9.9 \pm 0.5$  GtC in 2013 (Fig. 5), 2.3% (including leap year correction) higher than the emissions in 2012. This compares to our projection of 2.1% yr<sup>-1</sup> made last year (Le 15 Quéré et al., 2014), based on an estimated GDP growth of 2.9% yr<sup>-1</sup> and improvement in  $I_{\text{FF}}$  of  $-0.8\%$  yr<sup>-1</sup> (Table 9). The latest estimate of GDP growth for 2013 was 3.3% yr<sup>-1</sup> (IMF, 2014) and hence  $I_{\text{FF}}$  improved by  $-1.0\%$  yr<sup>-1</sup>, very close to our projection. The 2013 emissions were distributed among coal (43%), oil (33%), gas (18%), 20 cement (5.5%) and gas flaring (0.6%). The first four categories increased by 3.0, 1.4, 1.4 and 4.7% respectively over the previous year (including leap year adjustment). Due to lack of data gas flaring in 2012 and 2013 are assumed equal to 2011.

Using Eq. (6), we estimate that global fossil fuel CO<sub>2</sub> emissions in 2014 will reach  $10.1 \pm 0.6$  GtC ( $37.0 \pm 2.2$  GtCO<sub>2</sub>), or 2.5% above 2013 levels (likely range of 1.3– 25 3.5%; see Friedlingstein et al., 2014), and that emissions in 2014 will be 65% above emissions in 1990. The expected value is computed using the world GDP projection of 3.3% made by the IMF (2014) and a growth rate for  $I_{\text{FF}}$  of  $-0.7\%$  yr<sup>-1</sup> which is the

562

average from the previous 10 years. The  $I_{FF}$  is based on GDP in constant PPP (purchasing power parity) from the IEA (2013) up to 2011 (IEA/OECD, 2013) and extended using the IMF growth rates of 2.9% in 2012 and 3.3% in 2013. The uncertainty range is based on an uncertainty of 0.3% for GDP growth (the range in IMF estimates of 2014 GDP growth published in January, April, and July 2014 was 3.7, 3.6, and 3.4%, respectively) and the range in  $I_{FF}$  due to short-term trends of  $-0.7\% \text{ yr}^{-1}$  (2009–2013) and medium term trends of  $-1.0\% \text{ yr}^{-1}$  (1994–2013). The combined uncertainty range is therefore 1.2% (2.5–0.3–1.0; low GDP growth, large  $I_{FF}$  improvements) and 2.1% (2.5 + 0.3–0.7; high GDP growth, small  $I_{FF}$  improvements). Projections made in the previous global carbon budgets compared well to the actual  $\text{CO}_2$  emissions for that year (Table 9 and Fig. 9) and were useful to capture the current state of the fossil fuel emissions (see also Peters et al., 2013).

In 2013, global  $\text{CO}_2$  emissions were dominated by emissions from China (28%), the USA (14%), the EU (28 member states; 10%), and India (7%) compared to the global total including bunker fuels. These four regions account for 58% of global emissions. Growth rates for these countries from 2012 to 2013 were 4.2% (China), 2.9% (USA),  $-1.8\%$  (EU28), and 5.1% (India). The countries contributing most to the 2013 change in emissions were China (58% of the increase), USA (20% of the increase), India (17% of the increase), and EU28 (11% of the decrease). The per-capita  $\text{CO}_2$  emissions in 2013 were  $1.4 \text{ tC person}^{-1} \text{ yr}^{-1}$  for the globe, and were 4.5 (USA), 2.0 (China), 1.9 (EU28) and 0.5 (India)  $\text{tC person}^{-1} \text{ yr}^{-1}$  (Fig. 5e).

Territorial emissions in Annex B countries have remained stable from 1990–2012, while consumption emissions grew at  $0.5\% \text{ yr}^{-1}$  (Fig. 5c). In non-Annex B countries, territorial emissions, have grown at  $4.4\% \text{ yr}^{-1}$ , while consumption emissions have grown at  $4.1\% \text{ yr}^{-1}$ . In 1990, 62% of global territorial emissions were emitted in Annex B countries (34% in non-Annex B, and 4% in bunker fuels used for international shipping and aviation), while in 2012 this had reduced to 37% (58% in non-Annex B, and 6% in bunkers). In terms of consumption emissions this split was 63% in 1990 and 43% in 2012 (33 to 51% in non-Annex B). The difference between territorial and

consumption emissions (the net emission transfer via international trade) from non-Annex B to Annex B countries has increased from  $0.05 \text{ GtC yr}^{-1}$  in 1990 to  $0.46 \text{ GtC}$  in 2012 (Fig. 5), with an average annual growth rate of  $11\% \text{ yr}^{-1}$ . The increase in net emission transfers of  $0.41 \text{ GtC}$  from 1990–2012 compares with the emission reduction of  $0.27 \text{ GtC}$  in Annex B countries. These results clearly show a growing net emission transfer via international trade from non-Annex B to Annex B countries. In 2012, the biggest emitters from a consumption perspective were China (23% of the global total), USA (16%), EU28 (13%), and India (6%).

Based on DGVMs only, the global  $\text{CO}_2$  emissions from land-use change activities are estimated as  $0.9 \pm 0.6 \text{ GtC}$  in 2013, slightly below the 2004–2013 average of  $1.0 \pm 0.7 \text{ GtC yr}^{-1}$ . However, although the decadal mean generally agreed, the estimated annual variability was not consistent between the LUC-emissions estimated based on the combined bookkeeping method and fire-based estimate and the DGVMs, except that they are small relative to the variability from the residual land sink (Fig. 6a). This could be partly due to the design of the DGVM experiments, which use flux differences between simulations with and without land-cover change, and thus may overestimate variability e.g. due to fires in forest regions where the contemporary forest cover is smaller than pre-industrial cover used in the without land cover change runs. The extrapolated land cover input data for 2010–2013 may also explain part of the discrepancy, though it would not account for the larger variability in the DGVMs.

### 3.2.2 Partitioning

The atmospheric  $\text{CO}_2$  growth rate was  $5.4 \pm 0.2 \text{ GtC}$  in 2013 ( $2.53 \pm 0.09 \text{ ppm}$ ; Fig. 4; Dlugokencky and Tans, 2014). This is significantly above the 2004–2013 average of  $4.3 \pm 0.1 \text{ GtC yr}^{-1}$ , though the interannual variability in atmospheric growth rate is large.

The ocean  $\text{CO}_2$  sink was  $2.9 \pm 0.5 \text{ GtC yr}^{-1}$  in 2013, an increase of  $0.1 \text{ GtC yr}^{-1}$  over 2012 according to ocean models. Five of the seven ocean models produce an increase in the ocean  $\text{CO}_2$  sink in 2013 compared to 2012. However the two data products available over that period produce a decrease of  $-0.1 \text{ GtC yr}^{-1}$ . All estimates suggest



a maximum value of  $0.71 \text{ GtC yr}^{-1}$ , directly reflecting revisions in other terms of the budget, but still within the reported uncertainty.

Our capacity to separate the carbon budget components can be evaluated by comparing the land  $\text{CO}_2$  sink estimated through three approaches: (1) the budget residual ( $S_{\text{LAND}}$ ), which includes errors and biases from all components, (2) the land  $\text{CO}_2$  sink estimate by the DGVM ensemble, which are based on our understanding of processes of how the land responds to increasing  $\text{CO}_2$ , climate change and variability, and (3) the inverse model estimates which formally merge observational constraints with process-based models to close the global budget. These estimates are generally close (Fig. 6), both for the mean and for the interannual variability. The DGVM mean correlates with the budget residual with  $r = 0.71$  (Sect. 2.5.2; Fig. 6). The DGVMs produce a decadal mean and standard deviation across models of  $2.6 \pm 0.9 \text{ GtC yr}^{-1}$  for the period 2000–2009, nearly the same as the estimate produced with the budget residual (Table 7). *New insights from the comparison with the atmospheric inversions and their regional breakdown already provide a semi-independent way to validate the results.* It shows a first-order consistency but a lot of discrepancies, particularly for the allocation of the mean land sink between the tropics and the Northern Hemisphere. Understanding these discrepancies and further analysis of regional carbon budgets would provide additional information to quantify and improve our estimates, as has been undertaken by the REgional Carbon Cycle Assessment and Processes (Canadell et al., 2013).

Annual estimates of each component of the global carbon budgets have their limitations, some of which could be improved with better data and/or better understanding of carbon dynamics. The primary limitations involve resolving fluxes on annual time scales and providing updated estimates for recent years for which data-based estimates are not yet available or only beginning to emerge. Of the various terms in the global budget, only the fossil fuel burning and atmospheric growth rate terms are based primarily on empirical inputs supporting annual estimates in this carbon budget. The data on fossil fuel consumption and cement production are based on survey data in all countries. The other terms can be provided on an annual basis only through the use

of models. While these models represent the current state of the art, they provide only estimates of actual changes. For example, the decadal trends in global ocean uptake and the interannual variations associated with El Niño/La Niña (ENSO) are not directly constrained by observations, although many of the processes controlling these trends are sufficiently well known that the model-based trends still have value as benchmarks for further validation. Data-based products for the ocean  $\text{CO}_2$  sink provide new ways to evaluate the model results, and could be used directly as data become more rapidly available and methods for creating such products improve. Estimates of land-use emissions and their year-to-year variability have even larger uncertainty, and much of the underlying data are not available as an annual update. Efforts are underway to work with annually available satellite area change data or FAO reported data in combination with fire data and modelling to provide annual updates for future budgets. The best resolved changes are in atmospheric growth ( $G_{\text{ATM}}$ ), fossil fuel emissions ( $E_{\text{FF}}$ ), and by difference, the change in the sum of the remaining terms ( $S_{\text{OCEAN}} + S_{\text{LAND}} - E_{\text{LUC}}$ ). The variations from year-to-year in these remaining terms are largely model-based at this time. Further efforts to increase the availability and use of annual data for estimating the remaining terms with annual to decadal resolution are especially needed.

Our approach also depends on the reliability of the energy and land-cover change statistics provided at the country level, and are thus potentially subject to biases. Thus it is critical to develop multiple ways to estimate the carbon balance at the global and regional level, including estimates from the inversion of atmospheric  $\text{CO}_2$  concentration used here for the first time, the use of other oceanic and atmospheric tracers, and the compilation of emissions using alternative statistics (e.g. sectors). It is also important to challenge the consistency of information across observational streams, for example to contrast the coherence of temperature trends with those of  $\text{CO}_2$  sink trends. Multiple approaches ranging from global to regional scale would greatly help increase confidence and reduce uncertainty in  $\text{CO}_2$  emissions and their fate.

## 5 Conclusions

The estimation of global CO<sub>2</sub> emissions and sinks is a major effort by the carbon cycle research community that requires a combination of measurements and compilation of statistical estimates and results from models. The delivery of an annual carbon budget serves two purposes. First, there is a large demand for up-to-date information on the state of the anthropogenic perturbation of the climate system and its underpinning causes. A broad stakeholder community relies on the datasets associated with the annual carbon budget including scientists, policy makers, businesses, journalists, and the broader society increasingly engaged in adapting to and mitigating human-driven climate change. Second, over the last decade we have seen unprecedented changes in the human and biophysical environments (e.g. increase in the growth of fossil fuel emissions, ocean temperatures, and strength of the land sink), which call for more frequent assessments of the state of the Planet, and by implications a better understanding of the future evolution of the carbon cycle, and the requirements for climate change mitigation and adaptation. Both the ocean and the land surface presently remove a large fraction of anthropogenic emissions. Any significant change in the function of carbon sinks is of great importance to climate policymaking, as they affect the excess carbon dioxide remaining in the atmosphere and therefore the compatible emissions for any climate stabilization target. Better constraints of carbon cycle models against contemporary datasets raises the capacity for the models to become more accurate at future projections.

This all requires more frequent, robust, and transparent datasets and methods that can be scrutinized and replicated. After nine annual releases from the GCP, the effort is growing and the traceability of the methods has become increasingly complex. Here, we have documented in detail the datasets and methods used to compile the annual updates of the global carbon budget, explained the rationale for the choices made, the limitations of the information, and finally highlighted need for additional information where gaps exist.

569

This paper via “living data” will help to keep track of new budget updates. The evolution over time of the carbon budget is now a key indicator of the anthropogenic perturbation of the climate system, and its annual delivery joins a set of other climate indicators to monitor the evolution of human-induced climate change, such as the annual updates on the global surface temperature, sea level rise, minimum Arctic sea ice extent and others.

## 6 Data access

The data presented here are made available in the belief that their wide dissemination will lead to greater understanding and new scientific insights of how the carbon cycle works, how humans are altering it, and how we can mitigate the resulting human-driven climate change. The free availability of these data does not constitute permission for publication of the data. For research projects, if the data are essential to the work, or if an important result or conclusion depends on the data, co-authorship may need to be considered. Full contact details and information on how to cite the data are given at the top of each page in the accompanying database, and summarised in Table 2.

The accompanying database includes an Excel file organised in the following spreadsheets (accessible with the free viewer <http://www.microsoft.com/en-us/download/details.aspx?id=10>):

1. Summary
2. The global carbon budget (1959–2013)
3. Global CO<sub>2</sub> emissions from fossil fuel combustion and cement production by fuel type, and the per-capita emissions (1959–2013)
4. Territorial (e.g. as reported to the UN Framework Convention on Climate Change) country CO<sub>2</sub> emissions from fossil fuel combustion and cement production (1959–2013)

570

5. Consumption country CO<sub>2</sub> emissions from fossil fuel combustion and cement production and emissions transfer from the international trade of goods and services (1990–2012)
6. Emissions transfers (Consumption minus territorial emissions; 1990–2012)
- 5 7. CO<sub>2</sub> emissions from land-use change from the individual methods and models (1959–2013)
8. Ocean CO<sub>2</sub> sink from the individual ocean models and data products (1959–2013)
9. Terrestrial residual CO<sub>2</sub> sink from the DGVMs (1959–2013)
- 10 10. Additional information on the carbon balance prior to 1959 (1750–2013)
11. Country definitions

**The Supplement related to this article is available online at  
doi:10.5194/essdd-7-521-2014-supplement.**

*Acknowledgements.* We thank all people and institutions who provided the data used in this carbon budget, P. Cadule, C. Enright, J. Ghattas, G. Hurtt and S. Peng for support to the model simulations, D. Bakker for support to the interactions with the ocean CO<sub>2</sub> data community, F. Joos and S. Khaliwala for providing historical data, M. Heimann, G. McKinley and anonymous reviewer for their comments and suggestions. We thank E. Dlugokencky who provided the atmospheric CO<sub>2</sub> measurements and all those involved in collecting and providing the oceanographic CO<sub>2</sub> measurements used here, in particular for the ocean data for years 2012–2013 that are not included in SOCAT v2: J. Akl, S. Alin, M. Becker, R. Bott, R. D. Castle, R. Feely, J. Hare, C. Hunt, B. Huss, T. Ichikawa, A. Körtzinger, G. Lebon, S. Maenner, J. Mathis, W. McGillis, R. Morrison, D. Munro, S. Musielewicz, A. Nakadate, C. Neill, T. Newberger, A. Omar, C. Sabine, J. Salisbury, J. Shannahoff, I. Skjelvan, K. Sullivan, S. C. Sutherland, A. Sutton, C. Sweeney, C. Taylor, S. van Heuven, D. Vandemark and A. J. Watson. We

571

thank the institutions and funding agencies responsible for the collection and quality control of the data included in SOCAT, and the support of the International Ocean Carbon Coordination Project (IOCCP), the Surface Ocean Lower Atmosphere Study (SOLAS), and the Integrated Marine Biogeochemistry, Ecosystem Research program (IMBER) and UK Natural Environment Research Council (NERC) projects including National Capability, Ocean Acidification, Greenhouse Gases and Shelf Seas Biogeochemistry.

NERC provided funding to C. Le Quéré, R. Moriarty and the GCP through their International Opportunities Fund specifically to support this publication (NE/103002X/1), and to U. Schuster through UKOARP (NE/H017046/1). G. P. Peters and R. M. Andrews were supported by the Norwegian Research Council (236296). T. A. Boden was supported by US Department of Energy, Office of Science, Biological and Environmental Research (BER) programs under US Department of Energy contract DE-AC05-00OR22725. Y. Bozec was supported by Region Bretagne, CG29 and INSU (LEFE/MERMEX) for CARBORHONE cruises. J. G. Canadell and M. R. Raupach were supported by the Australian Climate Change Science Program. M. Hoppema received ICOS-D funding through German federal ministry of research BMBF to AWI (01 LK 1224). J. I. House was supported by a Leverhulme Early Career Fellowship. A. K. Jain was supported by the US National Science Foundation (NSF AGS 12-43071) the US Department of Energy, Office of Science and BER programs (DOE DE-SC0006706) and NASA LCLUC program (NASA NNX14AD94G). E. Kato was supported by the Environment Research and Technology Development Fund (S-10) of the Ministry of Environment of Japan. C. Koven was supported by the Director, Office of Science, Office of Biological and Environmental Research of the US Department of Energy under Contract No. DE-AC02-05CH11231 as part of their Regional and Global Climate Modelling Program. I. D. Lima was supported by the US National Science Foundation (NSF AGS-1048827). N. Metzl was supported by Institut National des Sciences de l'Univers (INSU) and Institut Paul Emile Victor (IPEV) for OISO cruises. A. Olsen was supported by the Centre for Climate Dynamics at the Bjerknes Centre for Climate Research. JE Salisbury was supported by grants from NOAA/NASA. T. Steinhoff was supported by ICOS-D (BMBF FK 01LK1101C). B. D. Stocker was supported by the Swiss National Science Foundation. A. J. Sutton was supported by NOAA. T. Takahashi was supported by grants from NOAA and the Comer Education and Science Foundation. B. Tilbrook was supported by the Australian Department of Environment and the Integrated Marine Observing System. A. Wiltshire was supported by the Joint UK DECC/Defra Met Office Hadley Centre Climate Programme (GA01101). A. Arneeth, P. Ciais, W. Peters, C. Le Quéré, and U. Schuster, S. Sitch and A. Wiltshire were sup-

572

ported by the EU FP7 for funding through projects GEOCarbon (283080). A. Arneeth, P. Ciais were also supported by COMBINE (226520). V. Kitidis, M. Hoppema, N. Metzl, C. Le Quéré, U. Schuster, J. Schwiger, J. Segsneider and T. Steinhoff were supported by the EU FP7 for funding through project CARBOCHANGE (264879). P. Friedlingstein, B. Poulter, P. Regnier and S. Sitch were supported by the EU FP7 for funding through projects LUC4C (GA603542). P. Friedlingstein was also supported by EMBRACE (GA282672). F. Chevallier and G. R. van der Werf were supported by the EU FP7 for funding through project MACC-II (283576). This is NOAA-PMEL contribution number 4216. Contributions from the Scripps Institution of Oceanography were supported by DOE grant DE-SC0005090, NSF grant ATM-1036399, and NOAA grant, NA10OAR4320156.

## References

- Andres, R., Boden, T., and Higdon, D.: A new evaluation of the uncertainty associated with CDIAC estimates of fossil fuel carbon dioxide emission, *Tellus B*, 66, 23616, doi:10.3402/tellusb.v66.23616, 2014.
- Andres, R. J., Fielding, D. J., Marland, G., Boden, T. A., Kumar, N., and Kearney, A. T.: Carbon dioxide emissions from fossil fuel use, 1751–1950, *Tellus*, 51, 759–765, 1999.
- Andres, R. J., Boden, T. A., Bréon, F.-M., Ciais, P., Davis, S., Erickson, D., Gregg, J. S., Jacobson, A., Marland, G., Miller, J., Oda, T., Olivier, J. G. J., Raupach, M. R., Rayner, P., and Treanton, K.: A synthesis of carbon dioxide emissions from fossil-fuel combustion, *Biogeosciences*, 9, 1845–1871, doi:10.5194/bg-9-1845-2012, 2012.
- Andrew, R. M. and Peters, G. P.: A multi-region input-output table based on the Global Trade Analysis Project Database (GTAP-MRIO), *Economic Systems Research*, 25, 99–121, 2013.
- Archer, D., Eby, M., Brovkin, V., Ridgwell, A., Cao, L., Mikolajewicz, U., Caldeira, K. M., K., Munhoven, G., Montenegro, A., and Tokos, K.: Atmospheric Lifetime of Fossil Fuel Carbon Dioxide, *Annu. Rev. Earth Pl. Sc.*, 37, 117–134, 2009.
- Assmann, K. M., Bentsen, M., Segsneider, J., and Heinze, C.: An isopycnic ocean carbon cycle model, *Geosci. Model Dev.*, 3, 143–167, doi:10.5194/gmd-3-143-2010, 2010.
- Atlas, R., Hoffman, R. N., Ardizzone, J., Leidner, S. M., Jusem, J. C., Smith, D. K., and Gombos, D.: A cross-calibrated, multiplatform ocean surface wind velocity product for meteorological and oceanographic applications, *B. Am. Meteorol. Soc.*, 92, 157–174, 2011.

573

- Aufdenkampe, A. K., Mayorga, E., Raymond, P. A., Melack, J. M., Doney, S. C., Alin, S. R., Aalto, R. E., and Yoo, K.: Riverine coupling of biogeochemical cycles between land, oceans and atmosphere, *Front. Ecol. Environ.*, 9, 53–60, 2011.
- Aumont, O. and Bopp, L.: Globalizing results from ocean in situ iron fertilization studies, *Global Biogeochem. Cy.*, 20, GB2017, doi:10.1029/2005GB002591, 2006.
- Baccini, A., Goetz, S. J., Walker, W. S., Laporte, N. T., Sun, M., Sulla-Menashe, D., Hackler, J., Beck, P. S. A., Dubayah, R., Friedl, M. A., Samanta, S., and Houghton, R. A.: Estimated carbon dioxide emissions from tropical deforestation improved by carbon-density maps, *Nature Climate Change*, 2, 182–186, 2012.
- Bakker, D. C. E., Pfeil, B., Smith, K., Hankin, S., Olsen, A., Alin, S. R., Cosca, C., Harasawa, S., Kozyr, A., Nojiri, Y., O'Brien, K. M., Schuster, U., Telszewski, M., Tilbrook, B., Wada, C., Akl, J., Barbero, L., Bates, N. R., Boutin, J., Bozec, Y., Cai, W.-J., Castle, R. D., Chavez, F. P., Chen, L., Chierici, M., Currie, K., de Baar, H. J. W., Evans, W., Feely, R. A., Fransson, A., Gao, Z., Hales, B., Hardman-Mountford, N. J., Hoppema, M., Huang, W.-J., Hunt, C. W., Huss, B., Ichikawa, T., Johannessen, T., Jones, E. M., Jones, S. D., Jutterström, S., Kitidis, V., Körtzinger, A., Landschützer, P., Lauvset, S. K., Lefèvre, N., Manke, A. B., Mathis, J. T., Merlivat, L., Metzl, N., Murata, A., Newberger, T., Omar, A. M., Ono, T., Park, G.-H., Paterson, K., Pierrot, D., Ríos, A. F., Sabine, C. L., Saito, S., Salisbury, J., Sarma, V. V. S. S., Schlitzer, R., Sieger, R., Skjelvan, I., Steinhoff, T., Sullivan, K. F., Sun, H., Sutton, A. J., Suzuki, T., Sweeney, C., Takahashi, T., Tjiputra, J., Tsurushima, N., van Heuven, S. M. A. C., Vandemark, D., Vlahos, P., Wallace, D. W. R., Wanninkhof, R., and Watson, A. J.: An update to the Surface Ocean CO<sub>2</sub> Atlas (SOCAT version 2), *Earth Syst. Sci. Data*, 6, 69–90, doi:10.5194/essd-6-69-2014, 2014.
- Ballantyne, A. P., Alden, C. B., Miller, J. B., Tans, P. P., and White, J. W. C.: Increase in observed net carbon dioxide uptake by land and oceans during the last 50 years, *Nature*, 488, 70–72, 2012.
- Bastviken, D., Tranvik, L. J., Downing, J. A., Crill, P. M., and Enrich-Prast, A.: Freshwater methane emissions offset the continental carbon sink, *Science*, 331, p. 50, doi:10.1126/science.1196808, 2011.
- Battin, T. J., Luysaert, S., Kaplan, L. A., Aufdenkampe, A. K., Richter, A., and Tranvik, L. J.: The boundless carbon cycle, *Nat. Geosci.*, 2, 598–600, 2009.
- Bauer, J. E., Cai, W.-J., Raymond, P. A., Bianchi, T. S., Hopkinson, C. S., and Regnier, P. A. G.: The changing carbon cycle of the coastal ocean, *Nature*, 504, 61–70, 2013.

574

- Best, M. J., Pryor, M., Clark, D. B., Rooney, G. G., Essery, R. L. H., Ménard, C. B., Edwards, J. M., Hendry, M. A., Porson, A., Gedney, N., Mercado, L. M., Sitch, S., Blyth, E., Boucher, O., Cox, P. M., Grimmond, C. S. B., and Harding, R. J.: The Joint UK Land Environment Simulator (JULES), model description – Part 1: Energy and water fluxes, *Geosci. Model Dev.*, 4, 677–699, doi:10.5194/gmd-4-677-2011, 2011.
- 5 Boden, T. A., Marland, G., and Andres, R. J.: Global, Regional, and National Fossil-Fuel CO<sub>2</sub> Emissions, Oak Ridge National Laboratory, U.S. Department of Energy, Oak Ridge, Tenn., USA, 2013.
- Borges, A. V. and Abril, G.: Carbon dioxide and methane dynamics in estuaries, in: *Treatise on Estuarine and Coastal Science*, edited by: Wolanski, E. and McLusky, D. S., Academic Press, 2011.
- 10 BP: Statistical Review of World Energy 2014, <http://www.bp.com/en/global/corporate/about-bp/energy-economics/statistical-review-of-world-energy.html>, last access: 8 August 2014.
- Bruno, M. and Joos, F.: Terrestrial carbon storage during the past 200 years: A monte carlo analysis of CO<sub>2</sub> data from ice core and atmospheric measurements, *Global Biogeochem. Cy.*, 11, 111–124, 1997.
- 15 Buitenhuis, E. T., Rivkin, R. B., Sailley, S., and Le Quéré, C.: Biogeochemical fluxes through microzooplankton, *Global Biogeochem. Cy.*, 24, GB4015, doi:10.1029/2009GB003601, 2010.
- Canadell, J. G., Le Quéré, C., Raupach, M. R., Field, C. B., Buitenhuis, E. T., Ciais, P., Conway, T. J., Gillett, N. P., Houghton, R. A., and Marland, G.: Contributions to accelerating atmospheric CO<sub>2</sub> growth from economic activity, carbon intensity, and efficiency of natural sinks, *P. Natl. Acad. Sci. USA*, 104, 18866–18870, 2007.
- 20 Canadell, J. G., Ciais, P., Sabine, C., and Joos, F. (Eds.): REgional Carbon Cycle Assessment and Processes (RECCAP), Special Issue, [http://www.biogeosciences.net/special\\_issue107.html](http://www.biogeosciences.net/special_issue107.html), 2013.
- Chevallier, F., Fisher, M., Peylin, P., Serrar, S., Bousquet, P., Bréon, F.-M., Chédin, A., and Ciais, P.: Inferring CO<sub>2</sub> sources and sinks from satellite observations: Method and application to TOVS data, *J. Geophys. Res.*, 110, D24309, doi:10.1029/2005JD006390, 2005.
- Ciais, P., Sabine, C., Govindasamy, B., Bopp, L., Brovkin, V., Canadell, J., Chhabra, A., DeFries, R., Galloway, J., Heimann, M., Jones, C., Le Quéré, C., Myneni, R., Piao, S., and Thornton, P.: Chapter 6: Carbon and Other Biogeochemical Cycles, in: *Climate Change 2013 The Physical Science Basis*, edited by: Stocker, T., Qin, D., and Plattner, G.-K., Cambridge University Press, Cambridge, 2013.

- Clark, D. B., Mercado, L. M., Sitch, S., Jones, C. D., Gedney, N., Best, M. J., Pryor, M., Rooney, G. G., Essery, R. L. H., Blyth, E., Boucher, O., Harding, R. J., Huntingford, C., and Cox, P. M.: The Joint UK Land Environment Simulator (JULES), model description – Part 2: Carbon fluxes and vegetation dynamics, *Geosci. Model Dev.*, 4, 701–722, doi:10.5194/gmd-4-701-2011, 2011.
- 5 Cole, J. J., Prairie, Y. T., Caraco, N. F., McDowell, W. H., Tranvik, L. J., Striegl, R. G., Duarte, C. M., Kortelainen, P., Downing, J. A., Middelburg, J. J., and Melack, J.: Plumbing the global carbon cycle: Integrating inland waters into the terrestrial carbon budget, *Ecosystems*, 10, 171–184, 2007.
- 10 Collins, W. J., Bellouin, N., Doutriaux-Boucher, M., Gedney, N., Halloran, P., Hinton, T., Hughes, J., Jones, C. D., Joshi, M., Liddicoat, S., Martin, G., O'Connor, F., Rae, J., Senior, C., Sitch, S., Totterdell, I., Wiltshire, A., and Woodward, S.: Development and evaluation of an Earth-System model – HadGEM2, *Geosci. Model Dev.*, 4, 1051–1075, doi:10.5194/gmd-4-1051-2011, 2011.
- 15 Cox, P. M., Betts, R. A., Jones, C. D., Spall, S. A., and Totterdell, I. J.: Acceleration of global warming due to carbon-cycle feedbacks in a coupled climate model, *Nature*, 408, 184–187, 2000.
- Danabasoglu, G., Yeager, S. G., Bailey, D., Behrens, E., Bentsen, M., Bi, D., Biastoch, A., Böning, C., Bozec, A., Canuto, V. M., Cassou, C., Chassignet, E., Coward, A. C., Danilov, S., Diansky, N., Drange, H., Farneti, R., Fernandez, E., Fogli, P. G., Forget, G., Fujii, Y., Griffies, S. M., Gusev, A., Heimbach, P., Howard, A., Jung, T., Kelley, M., Large, W. G., Leboissetier, A., Lu, J., Madec, G., Marsland, S. J., Masina, S., Navarra, A., Nurser, A. J. G., Pirani, A., Salas y Méliá, D., Samuels, B. L., Scheinert, M., Sidorenko, D., Treguier, A.-M., Tsujino, H., Uotila, P., Valcke, S., Voldoire, A., and Wangi, Q.: North Atlantic simulations in Coordinated Ocean-ice Reference Experiments phase II (CORE-II). Part I: Mean states, *Ocean Model.*, 25, 76–107, doi:10.1016/j.ocemod.2013.10.005, 2014.
- Davis, S. J. and Caldeira, K.: Consumption-based accounting of CO<sub>2</sub> emissions, *Proceedings of the National Academy of Sciences*, 107, 5687–5692, 2010.
- Davis, S. J., Peters, G. P., and Caldeira, K.: The supply chain of CO<sub>2</sub> emissions, *P. Natl. Acad. Sci.*, 108, 18554–18559, 2011.
- 30 Denman, K. L., Brasseur, G., Chidthaisong, A., Ciais, P., Cox, P. M., Dickinson, R. E., Hauglustaine, D., Heinze, C., Holland, E., Jacob, D., Lohmann, U., Ramachandran, S., Leite da Silva Dias, P., Wofsy, S. C., and Zhang, X.: Couplings Between Changes in the Climate Sys-

- tem and Biogeochemistry, Intergovernmental Panel on Climate Change, 978-0-521-70596-7, 499–587 pp., 2007.
- Dlugokencky, E. and Tans, P.: Trends in atmospheric carbon dioxide, National Oceanic & Atmospheric Administration, Earth System Research Laboratory (NOAA/ESRL), <http://www.esrl.noaa.gov/gmd/ccgg/trends>, last access: 8 August 2014.
- 5 Doney, S. C., Lima, I., Feely, R. A., Glover, D. M., Lindsay, K., Mahowald, N., Moore, J. K., and Wanninkhof, R.: Mechanisms governing interannual variability in upper-ocean inorganic carbon system and air–sea CO<sub>2</sub> fluxes: Physical climate and atmospheric dust, *Deep-Sea Res. PT II*, 56, 640–655, 2009.
- 10 Durant, A. J., Le Quééré, C., Hope, C., and Friend, A. D.: Economic value of improved quantification in global sources and sinks of carbon dioxide, *Phil. Trans. A*, 269, 1967–1979, 2010.
- Earles, J. M., Yeh, S., and Skog, K. E.: Timing of carbon emissions from global forest clearance, *Nature Climate Change*, 2, 682–685, 2012.
- El-Masri, B., Barman, R., Meiyappan, P., Song, Y., Liang, M., and Jain, A. K.: Carbon dynamics in the Amazonian Basin: Integration of eddy covariance and ecophysiological data with a land surface model, *Agr. Forest Meteorol.*, 182–183, 156–167, 2013.
- 15 Erb, K.-H., Kastner, T., Luysaert, S., Houghton, R. A., Kuemmerle, T., Olofsson, P., and Haberl, H.: Bias in the attribution of forest carbon sinks, *Nature Climate Change*, 3, 854–856, 2013.
- Etheridge, D. M., Steele, L. P., Langenfelds, R. L., and Francey, R. J.: Natural and anthropogenic changes in atmospheric CO<sub>2</sub> over the last 1000 years from air in Antarctic ice and firn, *J. Geophys. Res.*, 101, 4115–4128, 1996.
- 20 FAO: Global Forest Resource Assessment 2010, 378 pp., 2010.
- FAOSTAT: Food and Agriculture Organization Statistics Division, <http://faostat.fao.org/>, 2010.
- Francey, R. J., Trudinger, C. M., van der Schoot, M., Law, R. M., Krummel, P. B., Langenfelds, R. L., Steele, L. P., Allison, C. E., Stavert, A. R., Andres, R. J., and Rodenbeck, C.: Reply to 'Anthropogenic CO<sub>2</sub> emissions', *Nature Climate Change*, 3, 604–604, 2013.
- Friedlingstein, P., Houghton, R. A., Marland, G., Hackler, J., Boden, T. A., Conway, T. J., Canadell, J. G., Raupach, M. R., Ciais, P., and Le Quééré, C.: Update on CO<sub>2</sub> emissions, *Nat. Geosci.*, 3, 811–812, 2010.
- 30 Friedlingstein, P., Andrew, R. M., Rogelj, J., Peters, G. P., Canadell, J. G., Knutti, R., Luderer, G., Raupach, M. R., Schaeffer, M., van Vuuren, D. P., and Le Quééré, C.: Persistent growth of CO<sub>2</sub> emissions and implications for reaching climate targets, *Nat. Geosci.*, doi:10.1038/NGEO2248, 2014.

- Gasser, T. and Ciais, P.: A theoretical framework for the net land-to-atmosphere CO<sub>2</sub> flux and its implications in the definition of “emissions from land-use change”, *Earth Syst. Dynam.*, 4, 171–186, doi:10.5194/esd-4-171-2013, 2013.
- GCP: The Global Carbon Budget 2007, [http://lmacweb.env.uea.ac.uk/lequere/co2/2007/carbon\\_budget\\_2007.htm](http://lmacweb.env.uea.ac.uk/lequere/co2/2007/carbon_budget_2007.htm), last access: November 2013.
- 5 Giglio, L., Randerson, J. T., and van der Werf, G. R.: Analysis of daily, monthly, and annual burned area using the fourth-generation global fire emissions database (GFED4), *J. Geophys. Res.-Biogeo.*, 118, 317–328, doi:10.1002/jgrg.20042, 2013.
- Gitz, V. and Ciais, P.: Amplifying effects of land-use change on future atmospheric CO<sub>2</sub> levels, *Global Biogeochem. Cy.*, 17, 1024, doi:10.1029/2002GB001963, 2003.
- 10 Gregg, J. S., Andres, R. J., and Marland, G.: China: Emissions pattern of the world leader in CO<sub>2</sub> emissions from fossil fuel consumption and cement production, *Geophys. Res. Lett.*, 35, L08806, doi:10.1029/2007GL032887, 2008.
- Harris, I., Jones, P. D., Osborn, T. J., and Lister, D. H.: Updated high-resolution grids of monthly climatic observations – the CRU TS3.10 Dataset, *Int. J. Climatol.*, 34, 623–642, doi:10.1002/joc.3711, 2014.
- 15 Hertwich, E. G. and Peters, G. P.: Carbon Footprint of Nations: A Global, Trade-Linked Analysis, *Environ. Sci. Technol.*, 43, 6414–6420, doi:10.1021/es803496a, 2009.
- Houghton, R. A.: Revised estimates of the annual net flux of carbon to the atmosphere from changes in land use and land management 1850–2000, *Tellus B*, 55, 378–390, 2003.
- 20 Houghton, R. A., House, J. I., Pongratz, J., van der Werf, G. R., DeFries, R. S., Hansen, M. C., Le Quééré, C., and Ramankutty, N.: Carbon emissions from land use and land-cover change, *Biogeosciences*, 9, 5125–5142, doi:10.5194/bg-9-5125-2012, 2012.
- Hourdin, F., Musat, I., Bony, S., Braconnot, P., Codron, F., Dufresne, J.-L., Fairhead, L., Filiberti, M.-A., Freidlingstein, P., Grandpeix, J.-Y., Krinner, G., LeVan, P., Li, Z.-X., and Lott, F.: The LMDZ4 general circulation model: climate performance and sensitivity to parametrized physics with emphasis on tropical convection, *Clim. Dynam.*, 27, 787–813, 2006.
- 25 Hurtt, G. C., Chini, L. P., Frolking, S., Betts, R. A., Feddema, J., Fischer, G., Fisk, J. P., Hibbard, K., Houghton, R. A., Janetos, A., Jones, C. D., Kindermann, G., Kinoshita, T., Klein Goldewijk, K., Riahi, K., Shevliakova, E., Smith, S., Stehfest, E., Thomson, A., Thornton, P., van Vuuren, D. P., and Wang, Y. P.: Harmonization of land-use scenarios for the period 1500–2100: 600 years of global gridded annual land-use transitions, wood harvest, and resulting secondary lands, *Clim. Change*, 109, 117–161, 2011.
- 30

- IEA/OECD: CO<sub>2</sub> emissions from fuel combustion, Paris, 2013.
- Ilyina, T., Six, K., Segschneider, J., Maier-Reimer, E., Li, H., and Núñez-Riboni, I.: The global ocean biogeochemistry model HAMOCC: Model architecture and performance as component of the MPI-Earth System Model in different CMIP5 experimental realizations, *Journal of Advances in Modeling Earth Systems*, 5, 287–315, 2013.
- IMF: World Economic Outlook of the International Monetary Fund, <http://www.imf.org/external/ns/cs.aspx?id=29>, last access: 14 July 2014.
- Ito, A. and Inatomi, M.: Use of a process-based model for assessing the methane budgets of global terrestrial ecosystems and evaluation of uncertainty, *Biogeosciences*, 9, 759–773, doi:10.5194/bg-9-759-2012, 2012.
- Jacobson, A. R., Mikaloff Fletcher, S. E., Gruber, N., Sarmiento, J. L., and Gloor, M.: A joint atmosphere-ocean inversion for surface fluxes of carbon dioxide: 1. Methods and global-scale fluxes, *Global Biogeochem. Cy.*, 21, GB1019, doi:10.1029/2005GB002556, 2007.
- Jain, A. K., Meiyappan, P., Song, Y., and House, J. I.: CO<sub>2</sub> Emissions from Land-Use Change Affected More by Nitrogen Cycle, than by the Choice of Land Cover Data, *Global Change Biol.*, 9, 2893–2906, 2013.
- Joos, F. and Spahni, R.: Rates of change in natural and anthropogenic radiative forcing over the past 20,000 years, *P. Natl. Acad. Sci. USA*, 105, 1425–1430, 2008.
- Kato, E., Kinoshita, T., Ito, A., Kawamiya, M., and Yamagata, Y.: Evaluation of spatially explicit emission scenario of land-use change and biomass burning using a process-based biogeochemical model, *Journal of Land Use Science*, 8, 104–122, 2013.
- Keeling, C. D., Bacastow, R. B., Bainbridge, A. E., Ekdhal, C. A., Guenther, P. R., and Waterman, L. S.: Atmospheric carbon dioxide variations at Mauna Loa Observatory, Hawaii, *Tellus*, 28, 538–551, 1976.
- Keeling, R. F., Manning, A. C., and Dubey, M. K.: The atmospheric signature of carbon capture and storage, *Philos. T. Roy. Soc. A*, 369, 2113–2132, doi:10.1098/rsta.2011.0016, 2011.
- Khatiwala, S., Primeau, F., and Hall, T.: Reconstruction of the history of anthropogenic CO<sub>2</sub> concentrations in the ocean, *Nature*, 462, 346–350, 2009.
- Khatiwala, S., Tanhua, T., Mikaloff Fletcher, S., Gerber, M., Doney, S. C., Graven, H. D., Gruber, N., McKinley, G. A., Murata, A., Ríos, A. F., and Sabine, C. L.: Global ocean storage of anthropogenic carbon, *Biogeosciences*, 10, 2169–2191, doi:10.5194/bg-10-2169-2013, 2013.
- Kirschke, S., Bousquet, P., Ciais, P., Saunoy, M., Canadell, J. G., Dlugokencky, E. J., Bergamaschi, P., Bergmann, D., Blake, D. R., Bruhwiler, L., Cameron Smith, P., Castaldi, S., Cheval-

- lier, F., Feng, L., Fraser, A., Heimann, M., Hodson, E. L., Houweling, S., Josse, B., Fraser, P. J., Krummel, P. B., Lamarque, J., Langenfelds, R. L., Le Quééré, C., Naik, V., O'Doherty, S., Palmer, P. I., Pison, I., Plummer, D., Poulter, B., Prinn, R. G., Rigby, M., Ringeval, B., Santini, M., Schmidt, M., Shindell, D. T., Simpson, I. J., Spahni, R., Steele, L. P., Strode, S. A., Sudo, K., Szopa, S., van der Werf, G. R., Voulgarakis, A., van Weele, M., Weiss, R. F., Williams, J. E., and Zeng, G.: Three decades of global methane sources and sinks, *Nat. Geosci.*, 6, 813–823, 2013.
- Klein Goldewijk, K., Beusen, A., van Drecht, G., and de Vos, M.: The HYDE 3.1 spatially explicit database of human-induced global land-use change over the past 12,000 years, *Global Ecol. Biogeogr.*, 20, 73–86, 2011.
- Koven, C. D., Riley, W. J., Subin, Z. M., Tang, J. Y., Torn, M. S., Collins, W. D., Bonan, G. B., Lawrence, D. M., and Swenson, S. C.: The effect of vertically resolved soil biogeochemistry and alternate soil C and N models on C dynamics of CLM4, *Biogeosciences*, 10, 7109–7131, doi:10.5194/bg-10-7109-2013, 2013.
- Krinner, G., Viovy, N., de Noblet, N., Ogée, J., Friedlingstein, P., Ciais, P., Sitch, S., Polcher, J., and Prentice, I. C.: A dynamic global vegetation model for studies of the coupled atmosphere-biosphere system, *Global Biogeochem. Cy.*, 19, 1–33, 2005.
- Krumins, V., Gehlen, M., Arndt, S., Van Cappellen, P., and Regnier, P.: Dissolved inorganic carbon and alkalinity fluxes from coastal marine sediments: model estimates for different shelf environments and sensitivity to global change, *Biogeosciences*, 10, 371–398, doi:10.5194/bg-10-371-2013, 2013.
- Lamarque, J.-F., Bond, T. C., Eyring, V., Granier, C., Heil, A., Klimont, Z., Lee, D., Lioussé, C., Mieville, A., Owen, B., Schultz, M. G., Shindell, D., Smith, S. J., Stehfest, E., Van Aardenne, J., Cooper, O. R., Kainuma, M., Mahowald, N., McConnell, J. R., Naik, V., Riahi, K., and van Vuuren, D. P.: Historical (1850–2000) gridded anthropogenic and biomass burning emissions of reactive gases and aerosols: methodology and application, *Atmos. Chem. Phys.*, 10, 7017–7039, doi:10.5194/acp-10-7017-2010, 2010.
- Landschützer, P., Gruber, N., Bakker, D. C. E., and Schuster, U.: Recent variability of the global ocean carbon sink, *Global Biogeochem. Cy.*, 28, doi:10.1002/2014GB004853, 2014.
- Laruelle, G. G., Durr, H. H., Slomp, C. P., and Borges, A. V.: Evaluation of sinks and sources of CO<sub>2</sub> in the global coastal ocean using a spatially-explicit typology of estuaries and continental shelves, *Geophys. Res. Lett.*, 37, L15607, doi:10.1029/2010GL043691, 2010.
- Le Quééré, C.: Closing the global budget for CO<sub>2</sub>, *Global Change*, 74, 28–31, 2009.

- Le Quéré, C., Raupach, M. R., Canadell, J. G., Marland, G., Bopp, L., Ciais, P., Conway, T. J., Doney, S. C., Feely, R. A., Foster, P., Friedlingstein, P., Gurney, K., Houghton, R. A., House, J. I., Huntingford, C., Levy, P. E., Lomas, M. R., Majkut, J., Metzl, N., Ometto, J. P., Peters, G. P., Prentice, I. C., Randerson, J. T., Running, S. W., Sarmiento, J. L., Schuster, U., Sitch, S., Takahashi, T., Viovy, N., van der Werf, G. R., and Woodward, F. I.: Trends in the sources and sinks of carbon dioxide, *Nat. Geosci.*, 2, 831–836, 2009.
- Le Quéré, C., Andres, R. J., Boden, T., Conway, T., Houghton, R. A., House, J. I., Marland, G., Peters, G. P., van der Werf, G. R., Ahlström, A., Andrew, R. M., Bopp, L., Canadell, J. G., Ciais, P., Doney, S. C., Enright, C., Friedlingstein, P., Huntingford, C., Jain, A. K., Jourdain, C., Kato, E., Keeling, R. F., Klein Goldewijk, K., Levis, S., Levy, P., Lomas, M., Poulter, B., Raupach, M. R., Schwinger, J., Sitch, S., Stocker, B. D., Viovy, N., Zaehle, S., and Zeng, N.: The global carbon budget 1959–2011, *Earth Syst. Sci. Data*, 5, 165–185, doi:10.5194/essd-5-165-2013, 2013.
- Le Quéré, C., Peters, G. P., Andres, R. J., Andrew, R. M., Boden, T. A., Ciais, P., Friedlingstein, P., Houghton, R. A., Marland, G., Moriarty, R., Sitch, S., Tans, P., Arneeth, A., Arvanitis, A., Bakker, D. C. E., Bopp, L., Canadell, J. G., Chini, L. P., Doney, S. C., Harper, A., Harris, I., House, J. I., Jain, A. K., Jones, S. D., Kato, E., Keeling, R. F., Klein Goldewijk, K., Körtzinger, A., Koven, C., Lefèvre, N., Maignan, F., Omar, A., Ono, T., Park, G.-H., Pfeil, B., Poulter, B., Raupach, M. R., Regnier, P., Rödenbeck, C., Saito, S., Schwinger, J., Segsneider, J., Stocker, B. D., Takahashi, T., Tilbrook, B., van Heuven, S., Viovy, N., Wanninkhof, R., Wiltshire, A., and Zaehle, S.: Global carbon budget 2013, *Earth Syst. Sci. Data*, 6, 235–263, doi:10.5194/essd-6-235-2014, 2014.
- Manning, A. C. and Keeling, R. F.: Global oceanic and land biotic carbon sinks from the Scripps atmospheric oxygen flask sampling network, *Tellus B*, 58, 95–116, 2006.
- Marland, G.: Uncertainties in accounting for CO<sub>2</sub> from fossil fuels, *J. Ind. Ecol.*, 12, 136–139, 2008.
- Marland, G., Andres, R. J., Blasing, T. J., Boden, T. A., Broniak, C. T., Gregg, J. S., Losey, L. M., and Treanton, K.: Energy, industry and waste management activities: An introduction to CO<sub>2</sub> emissions from fossil fuels, in: A report by the US Climate Change Science Program and the Subcommittee on Global Change Research, in *The First State of the Carbon Cycle Report (SOCCR): The North American Carbon Budget and Implications for the Global Carbon Cycle*, edited by: King, A. W., Dilling, L., Zimmerman, G. P., Fairman, D. M., Houghton, R. A., Marland, G., Rose, A. Z., and Wilbanks, T. J., Asheville, NC, 2007.

- Marland, G., Hamal, K., and Jonas, M.: How Uncertain Are Estimates of CO<sub>2</sub> Emissions?, *J. Ind. Ecol.*, 13, 4–7, 2009.
- Masarie, K. A. and Tans, P. P.: Extension and integratio of atmospheric carbon dioxide data into a globally consistent measurement record, *J. Geophys. Res.-Atmos.*, 100, 11593–11610, 1995.
- McNeil, B. I., Matear, R. J., Key, R. M., Bullister, J. L., and Sarmiento, J. L.: Anthropogenic CO<sub>2</sub> uptake by the ocean based on the global chlorofluorocarbon data set, *Science*, 299, 235–239, 2003.
- Mercado, L. M., Bellouin, N., Sitch, S., Boucher, O., Huntingford, C., Wild, M., and Cox, P. M.: Impact of changes in diffuse radiation on the global land carbon sink, *Nature*, 458, 1014–1018, 2009.
- Mikaloff Fletcher, S. E., Gruber, N., Jacobson, A. R., Doney, S. C., Dutkiewicz, S., Gerber, M., Follows, M., Joos, F., Lindsay, K., Menemenlis, D., Mouchet, A., Müller, S. A., and Sarmiento, J. L.: Inverse estimates of anthropogenic CO<sub>2</sub> uptake, transport, and storage by the oceans, *Global Biogeochem. Cy.*, 20, GB2002, doi:10.1029/2005GB002530, 2006.
- Narayanan, B., Aguiar, A., and McDougall, R.: Global Trade, Assistance, and Production: The GTAP 8 Data Base, <http://www.gtap.agecon.purdue.edu/databases/v8/default.asp>, last access: September 2013.
- NOAA/ESRL: NOAA/ESRL calculation of global means, [http://www.esrl.noaa.gov/gmd/ccgg/about/global\\_means.html](http://www.esrl.noaa.gov/gmd/ccgg/about/global_means.html), last access: 8 August 2014.
- Oke, P. R., Griffin, D. A., Schiller, A., Matear, R. J., Fiedler, R., Mansbridge, J., Lenton, A., Cahill, M., Chamberlain, M. A., and Ridgway, K.: Evaluation of a near-global eddy-resolving ocean model, *Geosci. Model Dev.*, 6, 591–615, doi:10.5194/gmd-6-591-2013, 2013.
- Oleson, K., Lawrence, D., Bonan, G., Drewniak, B., Huang, M., Koven, C., Levis, S., Li, F., Riley, W., Subin, Z., Swenson, S., Thornton, P., Bozbiyik, A., Fisher, R., Heald, C., Kluzek, E., Lamarque, J., Lawrence, P., Leung, L., Lipscomb, W., Muszala, S., Ricciuto, D., Sacks, W., Tang, J., and Yang, Z.: Technical Description of version 4.5 of the Community Land Model (CLM), NCAR, 2013.
- Park, G. H., Wanninkhof, R., Doney, S. C., Takahashi, T., Lee, K., Feely, R. A., Sabine, C. L., Trinanés, J., and Lima, I. D.: Variability of global net sea-air CO<sub>2</sub> fluxes over the last three decades using empirical relationships, *Tellus B*, 62, 352–368, 2010.
- Peters, G. P. and Hertwich, E. G.: Post-Kyoto Greenhouse Gas Inventories: Production versus Consumption, *Climatic Change*, 2008. 51-66, 2008.

- Peters, G. P., Andrew, R., and Lennos, J.: Constructing a multi-regional input-output table using the GTAP database, *Economic Systems Research*, 23, 131–152, 2011a.
- Peters, G. P., Minx, J. C., Weber, C. L., and Edenhofer, O.: Growth in emission transfers via international trade from 1990 to 2008, *P. Natl. Acad. Sci. USA*, 108, 8903–8908, 2011b.
- 5 Peters, G. P., Davis, S. J., and Andrew, R.: A synthesis of carbon in international trade, *Biogeosciences*, 9, 3247–3276, doi:10.5194/bg-9-3247-2012, 2012a.
- Peters, G. P., Marland, G., Le Quéré, C., Boden, T. A., Canadell, J. G., and Raupach, M. R.: Correspondence: Rapid growth in CO<sub>2</sub> emissions after the 2008–2009 global financial crisis, *Nature Climate Change*, 2, 2–4, 2012b.
- 10 Peters, G. P., Andrew, R. M., Boden, T., Canadell, J. G., Ciais, P., Le Quéré, C., Marland, G., Raupach, M. R., and Wilson, C.: The challenge to keep global warming below 2 °C, *Nature Climate Change*, 3, 4–6, 2013.
- Peters, W., Krol, M. C., Van Der Werf, G. R., Houweling, S., Jones, C. D., Hughes, J., Schaefer, K., Masarie, K. A., Jacobson, A. R., Miller, J. B., Cho, C. H., Ramonet, M., Schmidt, M., Ciattaglia, L., Apadula, F., Heltai, D., Meinhardt, F., Di Sarra, A. G., Piacentino, S., Sferlazzo, D., Aalto, T., Hatakka, J., Ström, J., Haszpra, L., Meijer, H. A. J., Van Der Laan, S., Neubert, R. E. M., Jordan, A., Rodó, X., Morguí, J.-A., Vermeulen, A. T., Popa, E., Rozanski, K., Zimnoch, M., Manning, A. C., Leuenberger, M., Uglietti, C., Dolman, A. J., Ciais, P., Heimann, M. And Tans, P. P.: Seven years of recent European net terrestrial carbon dioxide exchange constrained by atmospheric observations, *Global Change Biol.*, 16, 1317–1337, 2010.
- 20 Peylin, P., Law, R. M., Gurney, K. R., Chevallier, F., Jacobson, A. R., Maki, T., Niwa, Y., Patra, P. K., Peters, W., Rayner, P. J., Rödenbeck, C., van der Laan-Luijkx, I. T., and Zhang, X.: Global atmospheric carbon budget: results from an ensemble of atmospheric CO<sub>2</sub> inversions, *Biogeosciences*, 10, 6699–6720, doi:10.5194/bg-10-6699-2013, 2013.
- 25 Pfeil, B., Olsen, A., Bakker, D. C. E., Hankin, S., Koyuk, H., Kozyr, A., Malczyk, J., Manke, A., Metz, N., Sabine, C. L., Akl, J., Alin, S. R., Bates, N., Bellerby, R. G. J., Borges, A., Boutin, J., Brown, P. J., Cai, W.-J., Chavez, F. P., Chen, A., Cosca, C., Fassbender, A. J., Feely, R. A., González-Dávila, M., Goyet, C., Hales, B., Hardman-Mountford, N., Heinze, C., Hood, M., Hoppema, M., Hunt, C. W., Hydes, D., Ishii, M., Johannessen, T., Jones, S. D., Key, R. M., Körtzinger, A., Landschützer, P., Lauvset, S. K., Lefèvre, N., Lenton, A., Laurantou, A., Merlivat, L., Midorikawa, T., Mintrop, L., Miyazaki, C., Murata, A., Nakadate, A., Nakano, Y., Nakaoka, S., Nojiri, Y., Omar, A. M., Padin, X. A., Park, G.-H., Paterson, K., Perez, F. F., Pierrot, D., Poisson, A., Ríos, A. F., Santana-Casiano, J. M., Salisbury, J., Sarma, V. V. S.

583

- S., Schlitzer, R., Schneider, B., Schuster, U., Sieger, R., Skjelvan, I., Steinhoff, T., Suzuki, T., Takahashi, T., Tedesco, K., Telszewski, M., Thomas, H., Tilbrook, B., Tjiputra, J., Vandemark, D., Veness, T., Wanninkhof, R., Watson, A. J., Weiss, R., Wong, C. S., and Yoshikawa-Inoue, H.: A uniform, quality controlled Surface Ocean CO<sub>2</sub> Atlas (SOCAT), *Earth Syst. Sci. Data*, 5, 125–143, doi:10.5194/essd-5-125-2013, 2013.
- 5 Pongratz, J., Reick, C. H., Raddatz, T., and Claussen, M.: Effects of anthropogenic land cover change on the carbon cycle of the last millennium, *Global Biogeochem. Cy.*, 23, GB4001, doi:10.1029/2009GB003488, 2009.
- Pongratz, J., Reick, C. H., Houghton, R. A., and House, J. I.: Terminology as a key uncertainty in net land use and land cover change carbon flux estimates, *Earth Syst. Dynam.*, 5, 177–195, doi:10.5194/esd-5-177-2014, 2014.
- 10 Poulter, B., Frank, D., Ciais, P., Myneni, R. B., Andela, N., Bi, J., Broquet, G., Canadell, J. G., Chevallier, F., Liu, Y. Y., Running, S. W., Sitch, S., and van der Werf, G. R.: Contribution of semi-arid ecosystems to interannual variability of the global carbon cycle, *Nature*, 509, 600–603, 2014.
- 15 Prather, M. J., Holmes, C. D., and Hsu, J.: Reactive greenhouse gas scenarios: Systematic exploration of uncertainties and the role of atmospheric chemistry, *Geophys. Res. Lett.*, 39, L09803, doi:10.1029/2012GL051440, 2012.
- Prentice, I. C., Farquhar, G. D., Fasham, M. J. R., Goulden, M. L., Heimann, M., Jaramillo, V. J., Khashgi, H. S., Le Quéré, C., Scholes, R. J., and Wallace, D. W. R.: The Carbon Cycle and Atmospheric Carbon Dioxide, in: *Climate Change 2001: The Scientific Basis. Contribution of Working Group I to the Third Assessment Report of the Intergovernmental Panel on Climate Change*, edited by: Houghton, J. T., Ding, Y., Griggs, D. J., Noguer, M., van der Linden, P. J., Dai, X., Maskell, K., and Johnson, C. A., Cambridge University Press, Cambridge, United Kingdom and New York, NY, USA., 2001.
- 25 Randerson, J., Chen, Y., van der Werf, G. R., Rogers, B. M., and Morton, D. C.: Global burned area and biomass burning emissions from small fires, *J. Geophys. Res.-Biogeo.*, 117, G04012, doi:10.1029/2012JG002128, 2012.
- Raupach, M. R., Marland, G., Ciais, P., Le Quéré, C., Canadell, J. G., Klepper, G., and Field, C. B.: Global and regional drivers of accelerating CO<sub>2</sub> emissions, *P. Natl. Acad. Sci. USA*, 104, 10288–10293, 2007.
- 30 Regnier, P., Friedlingstein, P., Ciais, P., Mackenzie, F. T., Gruber, N., Janssens, I. A., Laruelle, G. G., Lauerwald, R., Luysaert, S., Andersson, A. J., Arndt, S., Arnosti, C., Borges, A. V.,

584

- Dale, A. W., Gallego-Sala, A., Godd eris, Y., Goossens, N., Hartmann, J., Heinze, C., Ilyina, T., Joos, F., La Rowe, D. E., Leifeld, J., Meysman, F. J. R., Munhoven, G., Raymond, P. A., Spahni, R., Suntharalingam, P., and Thullner M.: Anthropogenic perturbation of the carbon fluxes from land to ocean, *Nat. Geosci.*, 6, 597–607, 2013.
- 5 Rhein, M., Rintoul, S. R., Aoki, S., Campos, E., Chambers, D., Feely, R. A., Gulev, S., Johnson, G. C., Josey, S. A., Kostianoy, A., Mauritzen, C., Roemmich, D., Talley, L. D., and Wang, F.: Chapter 3: Observations: Ocean, in: *Climate Change 2013 The Physical Science Basis*, Cambridge University Press, 2013.
- R odenbeck, C.: Estimating CO<sub>2</sub> sources and sinks from atmospheric mixing ratio measurements using a global inversion of atmospheric transport, Max Plank Institute, MPI-BGC, 10 2005.
- R odenbeck, C., Houweling, S., Gloor, M., and Heimann, M.: CO<sub>2</sub> flux history 1982–2001 inferred from atmospheric data using a global inversion of atmospheric transport, *Atmos. Chem. Phys.*, 3, 1919–1964, doi:10.5194/acp-3-1919-2003, 2003.
- 15 R odenbeck, C., Keeling, R. F., Bakker, D. C. E., Metzl, N., Olsen, A., Sabine, C., and Heimann, M.: Global surface-ocean pCO<sub>2</sub> and sea-air CO<sub>2</sub> flux variability from an observation-driven ocean mixed-layer scheme, *Ocean Sci.*, 9, 193–216, doi:10.5194/os-9-193-2013, 2013.
- R odenbeck, C., Bakker, D. C. E., Metzl, N., Olsen, A., Sabine, C., Cassar, N., Reum, F., Keeling, R. F., and Heimann, M.: Interannual sea-air CO<sub>2</sub> flux variability from an observation-driven 20 ocean mixed-layer scheme, *Biogeosciences*, 11, 4599–4613, doi:10.5194/bg-11-4599-2014, 2014.
- Rypdal, K., Paciomik, N., Eggleston, S., Goodwin, J., Irving, W., Penman, J., and Woodfield, M.: Chapter 1 Introduction to the 2006 Guidelines, in: *2006 IPCC Guidelines for National Greenhouse Gas Inventories*, edited by: Eggleston, S., Buendia, L., Miwa, K., Ngara, T., 25 and Tanabe, K., Institute for Global Environmental Strategies (IGES), Hayama, Kanagawa, Japan, 2006.
- Schimel, D., Alves, D., Enting, I., Heimann, M., Joos, F., Raynaud, D., Wigley, T., Prater, M., Derwent, R., Ehhalt, D., Fraser, P., Sanhueza, E., Zhou, X., Jonas, P., Charlson, R., Rodhe, H., Sadasivan, S., Shine, K. P., Fouquart, Y., Ramaswamy, V., Solomon, S., Srinivasan, J., 30 Albritton, D., Derwent, R., Isaksen, I., Lal, M., and Wuebbles, D.: Radiative Forcing of Climate Change, in: *Climate Change 1995 The Science of Climate Change. Contribution of Working Group I to the Second Assessment Report of the Intergovernmental Panel on Climate Change*, edited by: Houghton, J. T., Meira Rilho, L. G., Callander, B. A., Harris, N.,

- Kattenberg, A., and Maskell, K., Cambridge University Press, Cambridge, United Kingdom and New York, NY, USA, 1995.
- Scripps: The Keeling Curve, <http://keelingcurve.ucsd.edu/>, last access: 7 November 2013.
- S ef erian, R., Bopp, L., Gehlen, M., Orr, J., Eth e, C., Cadule, P., Aumont, O., Salas y M elia, D., 5 Voldoire, A. and Madec, G.: Skill assessment of three earth system models with common marine biogeochemistry, *Clim. Dynam.*, 40, 2549–2573, 2013.
- Shevliakova, E., Pacala, S., Malyshev, S., Hurtt, G., Milly, P., Caspersen, J., Sentman, L., Fisk, J., Wirth, C., and Crevoisier, C.: Carbon cycling under 300 years of land use change: Importance of the secondary vegetation sink, *Global Biogeochem. Cy.*, 23, GB2022, 10 doi:10.1029/2007GB003176, 2009.
- Sitch, S., Smith, B., Prentice, I. C., Arneth, A., Bondeau, A., Cramer, W., Kaplan, J. O., Levis, S., Lucht, W., Sykes, M. T., Thonicke, K., and Venevsky, S.: Evaluation of ecosystem dynamics, plant geography and terrestrial carbon cycling in the LPJ dynamic global vegetation model *Global Change Biol.*, 9, 161–185, 2003.
- 15 Smith, B., Prentice, I. C., and Sykes, M. T.: Representation of vegetation dynamics in the modelling of terrestrial ecosystems: comparing two contrasting approaches within European climate space, *Global Ecol. Biogeogr.*, 10, 621–637 doi:10.1046/j.1466-822X.2001.t01-1-00256.x, 2001.
- Stocker, B. D., Roth, R., Joos, F., Spahni, R., Steinacher, M., Zaehle, S., Bouwman, L., and 20 Prentice, I. C.: Multiple greenhouse-gas feedbacks from the land biosphere under future climate change scenarios, *Nature Climate Change*, 3, 666–672, 2013a.
- Stocker, T., Qin, D., and Platner, G.-K.: *Climate Change 2013 The Physical Science Basis*, Cambridge University Press, 2013b.
- Sweeney, C., Gloor, E., Jacobson, A. R., Key, R. M., McKinley, G., Sarmiento, J. L., and Wan- 25 ninkhof, R.: Constraining global air-sea gas exchange for CO<sub>2</sub> with recent bomb <sup>14</sup>C measurements, *Global Biogeochem. Cy.*, 21, GB2015, doi:10.1029/2006GB002784, 2007.
- Tans, P. and Keeling, R. F.: Trends in atmospheric carbon dioxide, National Oceanic & Atmospheric Administration, Earth System Research Laboratory (NOAA/ESRL) & Scripps Institution of Oceanography, <http://www.esrl.noaa.gov/gmd/ccgg/trends/> and <http://scrippsco2.ucsd.edu/>, last access: 8 August 2014.
- 30 Tjiputra, J. F., Roelandt, C., Bentsen, M., Lawrence, D. M., Lorentzen, T., Schwinger, J., Seland,  ., and Heinze, C.: Evaluation of the carbon cycle components in the Norwegian Earth









Table 6. Continued.

Data Products for Land-use Change Emissions			
Bookkeeping	Houghton et al. (2012)		no change
Fire-based emissions	van der Werf et al. (2010)		no change
Ocean Biogeochemistry Models			
NEMO-PlankTOM5	Buitenhuis et al. (2010) <sup>h</sup>		no change
LSCE	Aumont and Bopp (2006)		no change
CCSM-BEC	Doney et al. (2009)		no change
MICOM-HAMOCC	Assmann et al. (2010) <sup>i</sup>		no change
MPIOM-HAMOCC	Ilyina et al. (2013)		no change
CNRM	S��ferian et al. (2013) <sup>j</sup>		not applicable
CSIRO	Oke et al. (2013)		not applicable
Data Products for Ocean CO <sub>2</sub> Sink			
Landsch��tzer	Landsch��tzer et al. (2014)		not applicable
Park	Park et al. (2010) <sup>k</sup>		no change
R��denbeck	R��denbeck et al. (2014) <sup>l</sup>		no change
Atmospheric Inversions for total CO <sub>2</sub> fluxes (Land-use Change + Land + Ocean CO <sub>2</sub> sinks)			
Peters	Peters et al. (2010)		not applicable
R��denbeck	R��denbeck et al. (2003)		not applicable
MACC <sup>m</sup>	Chevallier et al. (2005)		not applicable

<sup>a</sup> Community Land Model 4.5;  
<sup>b</sup> see also El-Masri et al. (2013);  
<sup>c</sup> Joint UK Land Environment Simulator;  
<sup>d</sup> see also Best et al. (2011);  
<sup>e</sup> Lund-Potsdam-Jena;  
<sup>f</sup> only used for total land ( $E_{LUC} + S_{LAND}$ ) flux calculation of multi-model mean;  
<sup>g</sup> see also Ito and Inatomi (2012);  
<sup>h</sup> with no nutrient restoring below the mixed layer depth;  
<sup>i</sup> with updates to the physical model as described in Tjiputra et al. (2013);  
<sup>j</sup> Further information (e.g., physical evaluation) for CNRM model can be found in Danabasoglu et al. (2014);  
<sup>k</sup> using winds from Atlas et al. (2011);  
<sup>l</sup> updated version "s81\_v3.6gcp";  
<sup>m</sup> The MACCv13.1 CO<sub>2</sub> inversion system, initially described by Chevallier et al. (2005), relies on the global tracer transport model LMDZ (Hourdin et al., 2006; see also Supplement Peylin et al., 2013).

595

**Table 7.** Comparison of results from the bookkeeping method and budget residuals with results from the DGVMs and inverse estimates for the periods 1960–1969, 1970–1979, 1980–1989, 1990–1999, 2000–2009, last decade and last year available. All values are in GtC yr<sup>-1</sup>. The DGVM uncertainties represents  $\pm 1\sigma$  of results from the nine individual models, for the inverse models all three results are given where available.

	mean (GtC yr <sup>-1</sup> )						
	1960-1969	1970-1979	1980-1989	1990-1999	2000-2009	2004-2013	2013
Land-use change emissions ( $E_{LUC}$ )							
Bookkeeping method	1.5 ± 0.5	1.3 ± 0.5	1.4 ± 0.5	1.6 ± 0.5	1.0 ± 0.5	0.9 ± 0.5	0.9 ± 0.5
DGVMs	1.3 ± 0.5	1.2 ± 0.6	1.3 ± 0.6	1.8 ± 0.9	1.1 ± 0.7	1.0 ± 0.7	0.9 ± 0.6
Residual terrestrial sink ( $S_{LAND}$ )							
Budget residual	1.8 ± 0.7	1.8 ± 0.8	1.6 ± 0.8	2.7 ± 0.7	2.4 ± 0.8	2.9 ± 0.8	2.5 ± 0.9
DGVMs	1.1 ± 0.7	2.0 ± 0.8	1.6 ± 1.0	2.1 ± 0.9	2.4 ± 0.9	2.5 ± 1.0	2.4 ± 1.2
Total land fluxes ( $E_{LUC} + S_{LAND}$ )							
Budget ( $E_{FF} - G_{ATM} - S_{OCEAN}$ )	0.2 ± 0.5	0.4 ± 0.6	0.2 ± 0.6	1.1 ± 0.6	1.5 ± 0.6	2.0 ± 0.7	1.6 ± 0.7
DGVMs	-0.3 ± 0.8	0.7 ± 0.8	0.1 ± 0.7	0.1 ± 1.0	1.2 ± 0.9	1.4 ± 1.0	1.5 ± 1.2
Inversions (P/R/C)	-/-/-	-/-/-	-0.2 <sup>o</sup> /0.7 <sup>*</sup>	-1.1 <sup>o</sup> /1.7 <sup>*</sup>	-1.5 <sup>o</sup> /2.4 <sup>*</sup>	1.7 <sup>o</sup> /1.9 <sup>o</sup> /3.1 <sup>o</sup>	1.3 <sup>o</sup> /2.2 <sup>o</sup> /2.7 <sup>o</sup>

<sup>o</sup> Estimate are not corrected for the influence of river fluxes, which would reduce the fluxes by 0.45 GtC yr<sup>-1</sup> when neglecting the anthropogenic influence on land (Sect. 7.2.2). Note: Letters identify each of the three inversions (P for Peters, R for R  denbeck and C for Chevallier).

596





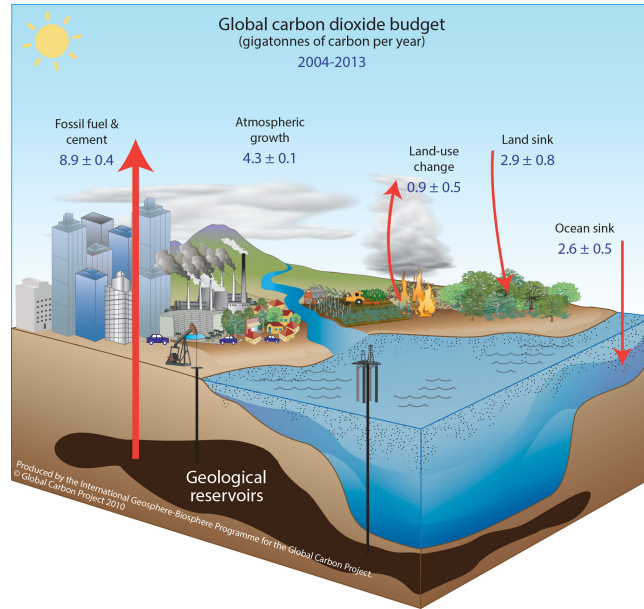


**Figure 2.** Schematic representation of the overall perturbation of the global carbon cycle caused by anthropogenic activities, averaged globally for the decade 2004–2013. The arrows represent emission from fossil fuel burning and cement production ( $E_{FF}$ ); emissions from deforestation and other land-use change ( $E_{LUC}$ ); the growth of carbon in the atmosphere ( $G_{ATM}$ ) and the uptake of carbon by the “sinks” in the ocean ( $S_{OCEAN}$ ) and land ( $S_{LAND}$ ) reservoirs. All fluxes are in units of  $GtC\ yr^{-1}$ , with uncertainties reported as  $\pm 1\sigma$  (68 % confidence that the real value lies within the given interval) as described in the text. This Figure is an update of one prepared by the International Geosphere Biosphere Programme for the GCP, first presented in Le Quéré (2009).

601

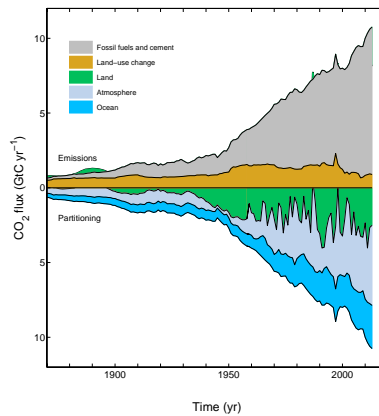


**Figure 3.** Combined components of the global carbon budget illustrated in Fig. 2 as a function of time, for (top) emissions from fossil fuel combustion and cement production ( $E_{FF}$ ; grey) and emissions from land-use change ( $E_{LUC}$ ; brown), and their partitioning among the atmosphere ( $G_{ATM}$ ; light blue), land ( $S_{LAND}$ ; green) and oceans ( $S_{OCEAN}$ ; dark blue). All time-series are in  $GtC\ yr^{-1}$ .  $G_{ATM}$  and  $S_{OCEAN}$  (and by construction also  $S_{LAND}$ ) prior to 1959 are based on different methods. The primary data sources are for: fossil fuel and cement emissions from Boden et al. (2013), with uncertainty of about  $\pm 5\%$  ( $\pm 1$ ); land-use change emissions from Houghton et al. (2012) with uncertainties of about  $\pm 30\%$ ; atmospheric growth rate prior to 1959 is from Joos and Spahni (2008) with uncertainties of about  $\pm 1$ – $1.5\ GtC\ decade^{-1}$  or  $\pm 0.1$ – $0.15\ GtC\ yr^{-1}$  (Bruno and Joos, 1997), and from Dlugokencky and Tans (2014) from 1959 with uncertainties of about  $\pm 0.2\ GtC\ yr^{-1}$ ; ocean sink prior to 1959 is from Khatiwala et al. (2013) with uncertainty of about  $\pm 30\%$ , and from this study from 1959 with uncertainties of about  $\pm 0.5\ GtC\ yr^{-1}$ ; residual land sink is obtained by difference (Eq. 8), resulting in uncertainties of about  $\pm 50\%$  prior to 1959 and  $\pm 0.8\ GtC\ yr^{-1}$  after that. See the text for more details of each component and their uncertainties.

602

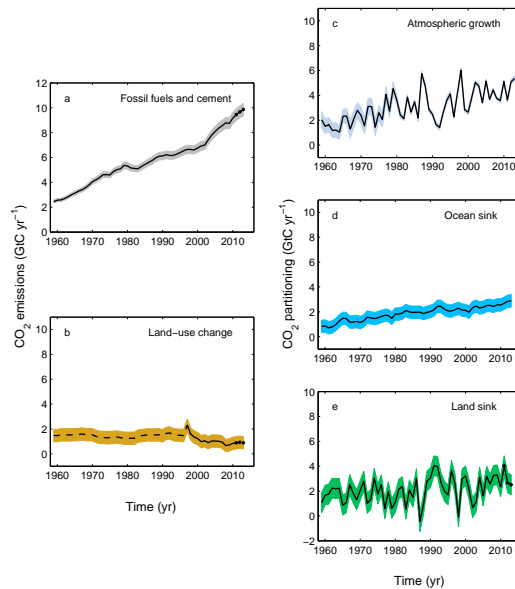
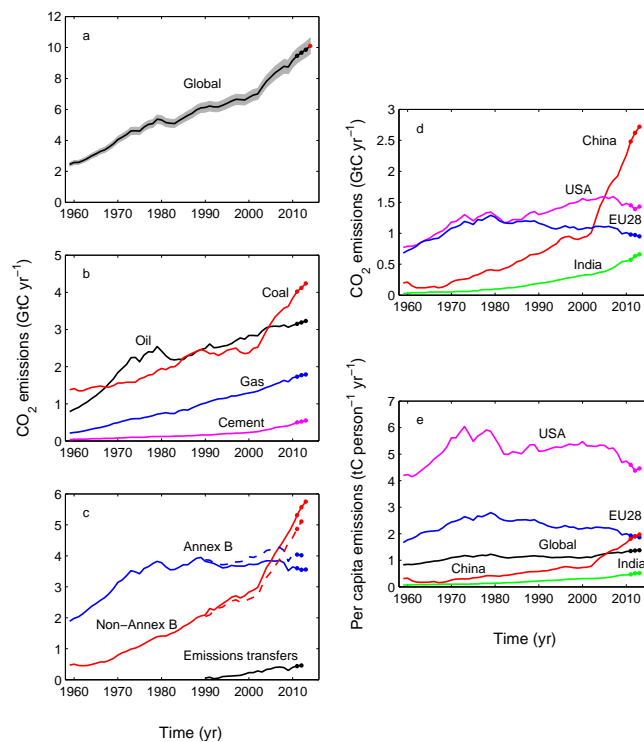


**Figure 4.** Components of the global carbon budget and their uncertainties as a function of time, presented individually for **(a)** emissions from fossil fuel combustion and cement production ( $E_{FF}$ ), **(b)** emissions from land-use change ( $E_{LUC}$ ), **(c)** atmospheric  $CO_2$  growth rate ( $G_{ATM}$ ), **(d)** the ocean  $CO_2$  sink ( $S_{OCEAN}$ , positive indicates a flux from the atmosphere to the ocean), and **(e)** the land  $CO_2$  sink ( $S_{LAND}$ , positive indicates a flux from the atmosphere to the land). All time-series are in  $GtC\ yr^{-1}$  with the uncertainty bounds representing  $\pm 1\sigma$  in shaded colour. Data sources are as in Fig. 2. The black dots in **(a)**, **(b)** and **(e)** show values for 2011, 2012 and 2013, that originate from a different dataset to the remainder of the data, as explained in the text.

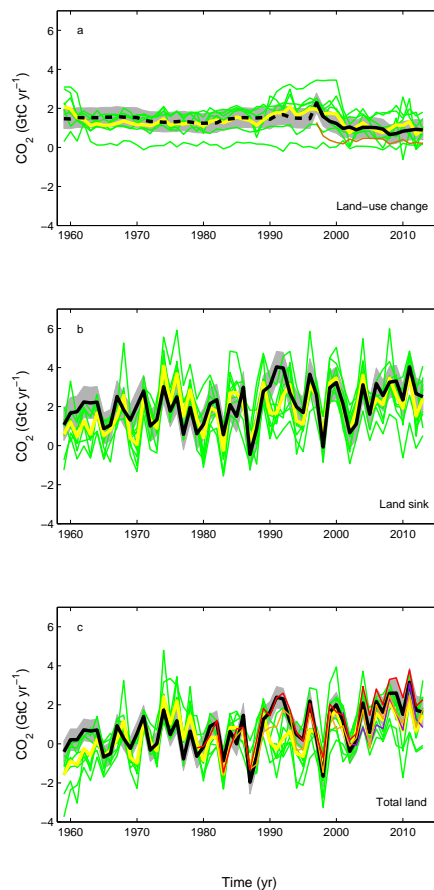
603



604

**Figure 5.** CO<sub>2</sub> emissions from fossil fuel combustion and cement production for **(a)** the globe, including an uncertainty of ±5% (grey shading), the emissions extrapolated using BP energy statistics (black dots) and the emissions projection for year 2014 based on GDP projection (red dot), **(b)** global emissions by fuel type, including coal (red), oil (black), gas (blue), and cement (purple), and excluding gas flaring which is small (0.6% in 2013), **(c)** territorial (full line) and consumption (dashed line) emissions for the countries listed in the Annex B of the Kyoto Protocol (blue lines; mostly advanced economies with emissions limitations) versus non-Annex B countries (red lines), also shown are the emissions transfer from non-Annex B to Annex B countries (black line) **(d)** territorial CO<sub>2</sub> emissions for the top three country emitters (USA – purple; China – red; India – green) and for the European Union (EU; blue for the 28 member states of the EU in 2012), and **(e)** per-capita emissions for the top three country emitters and the EU (all colours as in **d**) and the world (black). In **(b)** to **(e)**, the dots show the data that were extrapolated from BP energy statistics for 2011, 2012 and 2013. All time-series are in GtC yr<sup>-1</sup> except the per-capita emissions **(e)**, which are in tonnes of carbon per person per year (tC person<sup>-1</sup> yr<sup>-1</sup>). All territorial emissions are primarily from Boden et al. (2013) as detailed in the text; consumption-based emissions are updated from Peters et al. (2011a).

605



606



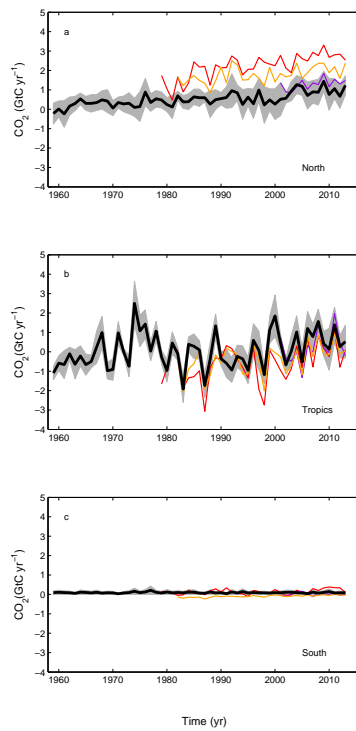


**Figure 8.** Surface CO<sub>2</sub> flux by latitude bands for the North (top panel, north of 30° N), Tropics (middle panel, 30° S–30° N), and South (south of 30° S). Estimates from the combination of the multi-model means for the land and oceans are shown (black) with  $\pm 1\sigma$  of the model ensemble (in grey). Results from the three atmospheric inversions are shown (MACC, v13.1 (Chevallier, 2005) in red; Rödenbeck et al. (2003) in orange; Peters et al. (2010) in purple; Table 6).

609

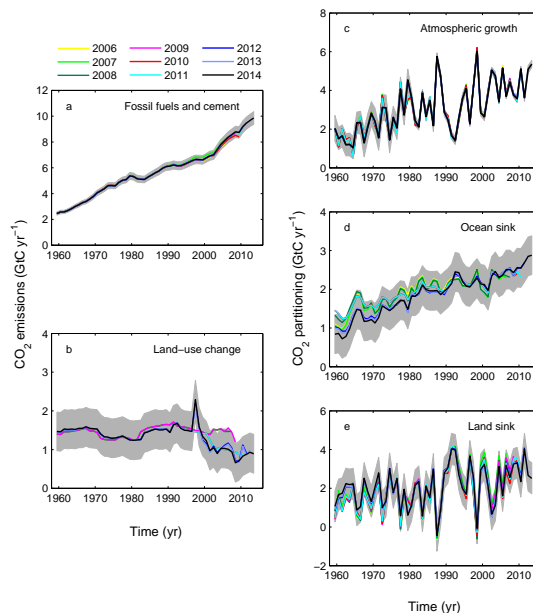


**Figure 9.** Comparison of global carbon budget components released annually by GCP since 2006. CO<sub>2</sub> emissions from both (a) fossil fuel combustion and cement production ( $E_{FF}$ ), and (b) land-use change ( $E_{LUC}$ ), and their partitioning among (c) the atmosphere ( $G_{ATM}$ ), (d) the ocean ( $S_{OCEAN}$ ), and (e) the land ( $S_{LAND}$ ). See legend for the corresponding years, with the 2006 carbon budget from Raupach et al. (2007); 2007 from Canadell et al. (2007); to 2008 published online only; 2009 from Le Quéré et al. (2009); 2010 from Friedlingstein et al. (2010); 2011 from Peters et al. (2012b); 2012 from Le Quéré et al. (2013); 2013 from Le Quéré et al. (2014) and this year's budget (2014). The budget year generally corresponds to the year when the budget was first release. All values are in  $\text{GtC yr}^{-1}$ .

610